THE DESIGN AND CONSTRUCTION OF A RECORDING SPECTROMETER FOR THE MEASUREMENT OF FLUORESCENCE EXCITATION SPECTRA IN THE VACUUM ULTRA-VIOLET REGION.

by

A.T. DAVIDSON B.Sc.Hons.

A Thesis presented for the Degree of Master of Science at Rhodes University, Grahamstown.

Department of Physics,
Rhodes University,
Grahamstown.

February 1963.

SUMMARY

A recording spectrometer for the measurement of fluorescence excitation spectra in the visible and ultra-violet regions of the spectrum is described. A direct method of modulating the hydrogen light source of the spectrograph is presented, whereby the discharge is driven by an A.C. power oscillator. The use of tuned amplifiers in the detecting unit is investigated as a means of eliminating the D.C. component of the dark current. Aspects of the modulation method are discussed.

Fluorescence and energy transfer in aromatic hydrocarbon is discussed with particular regard to anthracene. Some absorption, fluorescence, excitation and reflection spectra of anthracene obtained by previous workers are presented, together with Tables listing the wavelengths of principal maxima for the above spectra published in the literature. Features of the excitation spectrum of anthracene are discussed and are related to its absorption and fluorescence spectra. The role of surface effects, defects and impurities are discussed in relation to the fluorescence of anthracene.

The method of A.C. detection was unable to resolve the excitation spectrum of anthracene due to the high noise level associated with the method. However, peaks in the ultra-violet region of the hydrogen molecular spectrum were recorded at a modulation frequency of 400 Kc/sec. The noise level is explained and ways of improving the signal to noise ratio of the A.C. detection system are suggested. It is concluded that D.C. detection is a simpler and more direct way of measuring excitation spectra. No modulated signals were detected when the hydrogen discharge was excited at 6·5 Mc/sec. Signals were recorded at modulation frequencies of 400 Kc/sec. The degree of modulation at 400 Kc/sec. increased with decrease in the pressure of the hydrogen discharge.

ACKNOWLEDGEMENTS.

My sincere thanks go to the following persons for the ready assistance they gave me during the course of the work.

Professor J.A. Gledhill — for his interest, help and useful criticism.

Dr E.E. Baart — for his able direction, assistance and encouragement.

Messrs A.R. Ross-Scanlen, A. Eichstadt and G. Walters — for their valuable help from the workshop.

Professor J.A.V. Fairbrother, Mr A.S. Driver and Mr J.A.P. Phelps of Natal University, Pietermaritzburg, for the construction of a component of the vacuum system, and to Mr Driver for his interest and help in the project.

Mr J.W. West — of the University Workshop for the use of equipment to make part of the apparatus.

The South African Council for Scientific and Industrial Research for a grant, renewed for a second year, to carry out the work.

My Research Colleagues and Friends, of the Physics Department.

Reference sources have been acknowledged in the text. Otherwise, the work described in this thesis is to the best of my knowledge, original.

CONTENTS

TABLES, DIAGRAMS AND PLATES.

Chapter 1

INTRODUCTION

1.1 Electronic Processes in Aromatic Hydrocarbons.

A study of the optical properties of certain substances can yield information about the internal structure and energy states of the substance, and can also give information concerning the binding forces between molecules making up the material. The technique involves subjecting the substance to electromagnetic radiation or to charged particles, and measuring the effects of the interaction. The aromatic hydrocarbons form a convenient group for this type of investigation as they absorb visible and ultra-violet radiation and generally emit a characteristic luminescence after excitation. This work will be limited to aromatic hydrocarbons of the type $C_{4n+2}\ H_{2n+4}$, and in particular to anthracene $n = 3$. The group is built up of benzene rings fused together in a long chain with the number of rings increasing as the order of the series increases.

When radiation is absorbed by a substance, the energy may be dissipated in various ways. The molecule which has been excited may radiate the excess energy in the form of light, it may transfer the energy to a neighbouring molecule, it may dissociate, or it may return to the ground state by a non-radiative mechanism. The life-time of an undisturbed,

excited atom is usually about 10^{-7} sec, after this period it re-radiates its energy (1.1). Collisions may rob the atom of its excitation energy converting it into thermal motion, so that re-radiation of absorbed light usually occurs only under conditions of low pressure in the gaseous state. Certain aromatic hydrocarbons re-emit a portion of their absorbed energy in the form of light of longer wavelength. This luminescent radiation whether it be of long duration (phosphorescence), or of short duration (fluorescence), has distinctive properties. Only light emitted during the transition from the first electronic excited state to the ground state of the molecule has yet been observed (1.2). Defining the fluorescence or emission spectrum as the intensity of the wavelength components of the fluorescent light, then the structure of the fluorescence spectrum has been found to be practically independent of the wavelength of the exciting radiation. Also, the energy distribution in the fluorescence spectrum is independent of the wavelength of the exciting light. This is the case for practically all fluorescent compounds (1.3). Recently a red shift of the fluorescence spectrum with increasing energy of absorbed radiation has been reported for anthracene vapour (1.4), but this will be discussed in the next section.

It is usual to define the quantum efficiency of a luminescent material as the ratio of the number of luminescence

quanta emitted, to the number of incident quanta absorbed by the substance in an equal time interval. Two main theories have been proposed to explain why the fluorescence spectrum is independent of the exciting wavelength down to at least 2500 A.U. which, in the case of anthracene, is well into the second and higher electronic absorption bands. Perhaps the most widely held theory follows Pringsheim who favours a highly efficient process of internal conversion from the higher electronic states into the first electronic state, from which the observed emission occurs. Internal conversion occurs when the potential surface of the excited state intersects or approaches close to that of a lower excited state. The electron in the excited state then loses its excess energy as heat in reverting back to the lowest excited state.

An alternative model has been proposed by Birks (1.5), to explain why in absorption, transitions from the ground state to the second and higher electronic bands occur, while in emission only transitions from the first electronic state to the ground state appear to be allowed. It is a model of photon cascade whereby the higher excited states actually emit photons, the occurrence of which is hidden by strong reabsorption by neighbouring molecules. The cascade process continues with accompanying thermal degradation of the excess energy until the transparent region of the substance is reached, when the normal fluorescence from the first excited

state is visible. This theory may be valid for deep excitation by ionizing radiation, but for ultra-violet radiation which is strongly absorbed at the surface of hydrocarbon crystals, no short wave fluorescence has yet been detected. There is an exception to this, as fluorescence from the second excited state to the ground state has been reported for azulene (1.6). However this involved the sensitized fluorescence of azulene in a naphthalene solid solution, which requires a non-radiative mechanism of energy transfer.

It is known that excitation energy is transferred from solvent to solute molecules in certain organic solutions (1.7), and in certain mixed organic crystals (1.8), on excitation by ultra-violet light. The photon cascade theory is well suited to explain this. In liquid organic phosphors, the initial process would be the excitation of the solvent molecules leading to fluorescence emission which is absorbed and then re-emitted by the solute molecules. However, Furst and Kallman (1.7b) have shown that the photon cascade process only occurs in solutions containing several fluorescent solutes. It is not responsible for the migration of excitation energy from solvent to solute. Transfer is likely to occur by a radiationless process as at low concentrations, it is necessary to postulate a transfer mechanism which allows energy to move through a large number of molecules. Lipsky and Burton (1.9) favour a

mechanism whereby the solvent contains small ordered regions within which exciton transfer can occur, so that the whole region and not just the excited molecule is open to quenching by foreign molecules or to charge transfer.

In the case of certain hydrocarbon crystals, also, the emitting and absorbing centres do not necessarily coincide. Wright (1.10) has shown that impurity molecules on the surface of anthracene crystals have the effect of quenching the anthracene fluorescence and that there must be a migration of excitation energy through the crystal lattice to the quenching centre. He favours a radiationless resonance exchange process arising from overlap of the electron orbitals of the excited and unexcited molecule. Two other types of radiationless exchange are possible; electron migration and exciton migration. The transfer process by electron migration can be discarded, as in insulating crystals like the aromatic hydrocarbons, the excitation energy is usually well below the ionization level required to produce free electrons. The exciton mechanism of energy transfer was rejected by Wright (1.10) on the grounds that it required stronger coupling between molecules than actually occurs in the aromatic hydrocarbons. However, the exciton or non-conducting excited state, is known to occur in certain insulating crystals; and, in weakly bound solids such as anthracene, the exciton is an excited atom or molecule which

immediately hands on its energy to a neighbour (1.11). Exciton absorption of light can be regarded as a quantum transition in which a photon is absorbed with the formation of an exciton region, resulting in delocalization of energy over the dimensions of the region.

It is now generally accepted that the transfer of excitation energy in aromatic hydrocarbon crystals is by resonance transfer, or by exciton movement (1.12) (1.13). Sidman has shown that excitons can be trapped by lattice imperfections (1.14). The life-time of an exciton may also be terminated by the spontaneous emission of radiation. In certain cases, an exciton may be trapped by an impurity which may subsequently radiate the excess energy with a spectrum characteristic of the impurity. For transfer by resonance exchange, radiation may occur from "displaced" molecules in the crystal, or the transfer may be stopped by the removal of excess vibrational energy from the excited molecule in the form of heat.

The transition causing fluorescence in the aromatic hydrocarbons is thought to be by π electrons which play only a small part in the coupling forces between atoms. The $4n+2$ carbon atoms constituting the molecule each contribute one loosely bound π electron to the system. Good approximations to the energy levels of the aromatic hydrocarbons have been obtained by considering only the wave functions

of the π electrons present in the molecule when solving the wave equation (1.15).

1.2 Absorption, Fluorescence and Excitation Spectra.

The absorption spectrum of a substance is usually presented as the variation of the logarithm of the absorption coefficient of the substance with the wavelength of the exciting radiation. For the aromatic hydrocarbons, peaks in the visible and ultra-violet regions of the spectrum indicate transitions from the ground state to first and higher electronic energy levels. The fluorescence spectrum has already been defined and is practically independent of the exciting wavelength for this class of material. An excitation spectrum is defined as the variation of the fluorescent light intensity emitted by a substance with the wavelength of the exciting radiation. The excitation spectrum of crystalline anthracene has been investigated by Wright (1.16) and by Driver (1.17). Wright explained the variation of the integrated fluorescence with exciting wavelength, and established a correlation between minima in the excitation spectrum and maxima in the absorption spectrum.

The excitation spectra discussed by Wright were obtained by measuring the intensity of fluorescence transmitted through an anthracene crystal on irradiation by visible light. The light output at a certain excitation wavelength

was compared with the light emitted by a layer of sodium salicylate at the same wavelength. Sodium salicylate has a constant quantum efficiency over the wavelength range 800 A.U. to 3200 A.U. (1.18), and variation of the relative excitation spectrum reveals an apparent variation in the quantum efficiency of the anthracene crystal with exciting wavelength. For anthracene, most of the exciting light is absorbed at the crystal surface, but some light which is less strongly absorbed excites molecules deeper in the crystal. Therefore, the intensity of fluorescence escaping through the crystal surface from excited molecules near the surface, will be greater than from molecules excited deeper in the crystal, especially for substances which reabsorb their molecular fluorescence. Hence the excitation spectrum, measured after the remaining fluorescent light has travelled through the crystal, shows a minimum where the absorption spectrum shows a maximum and vice versa. This is the case in anthracene crystals which reabsorb 3/4 of their molecular fluorescence. In addition to providing the positions of the absorption maxima, the excitation spectrum allows an estimate to be made of relative absorption strengths.

There are other possible causes for the excitation spectrum. It is possible that the efficiency of the emission process itself changes when the exciting light

lies within the normal emission region of the crystal. Also, delayed or phosphorescent emission might have an effect on the excitation spectrum. A factor to be considered is the experimental method used to obtain the excitation spectrum. Generally, the fluorescence emission of the sample which falls within the sensitivity range of a photomultiplier is measured and compared with the fluorescence of a standard phosphor at the same exciting wavelength. This is valid provided the structure of the fluorescence spectrum of the sample is independent of the exciting wavelength. If there is a change in structure, the photomultiplier would not necessarily give the same reading for the integrated fluorescence of the sample, as the response of photomultipliers varies non-linearly with wavelength. The structure of the fluorescence spectrum of crystalline benzene has been shown to be independent of the means of excitation (1.3), and this should also apply to its derivatives, the aromatic hydrocarbons.

However, Stevens and Hutton (1.4) have reported a slight red shift of the fluorescence spectra of anthracene vapour with decreasing wavelength of excitation. This was accompanied by a loss of vibrational structure. At the same time there was a change in the relative intensity of the spectral components of the fluorescence with pressure. These changes would introduce variations in the excitation

spectra which might be attributed to other causes. Small variations in pressure should have negligible effect on molecules in the crystalline state and the corresponding change in the fluorescence spectrum can be neglected in this case. The red shift and loss of vibrational structure with increasing energy of absorbed quanta may, however, occur in the crystalline state as well. Emission bands of crystalline anthracene occur at wavelengths 3600 A.U. and 4150 A.U. [cf. Table II]. For a DUMONT photomultiplier tube whose spectral response covers the range 3200 A.U. to 5800 A.U. with maximum sensitivity at 4800 A.U.; an appreciable red shift of the 3600 A.U. band would cause an increase in the value obtained for the integrated emission which is not due to an increase of the crystal fluorescence, but is due to the characteristics of the photomultiplier. Therefore at shorter exciting wavelengths, a general increase in the measured fluorescence emission might result.

Variations in the quantum efficiency of sodium salicylate at wavelengths below 2500 A.U. have been reported (1.19), and would affect the relative excitation spectrum. It has also been reported that the quantum efficiency passes through a maximum at 2700 A.U. for thick layers of sodium salicylate (1.20). This would cause a minimum in the relative excitation spectra at that wavelength. However, the constant quantum efficiency of sodium salicylate has been confirmed

in the range 1800 A.U. to 2600 A.U. (1.21), and it would seem that provided thin layers are used, excitation spectra relative to sodium salicylate, should accurately represent the absolute excitation spectrum of the phosphor. Excitation spectra are also sensitive to variations of reflection coefficients with the incident wavelength exciting the phosphor, and it will be shown in the next section that selective reflection of the incident light tends to oppose variations in the excitation spectrum.

Excitation spectra are interpreted as arising out of self-absorption in crystals where there is overlap of absorption and fluorescence bands. This reduces the quantum efficiency of fluorescence and enhances the surface escape of fluorescence (1.16), causing a variation in the total fluorescence transmitted through the crystal. Support would be given to Wright's theory if it could be shown that the excitation spectra of micro-crystalline anthracene, which has negligible self-absorption, are independent of wavelength.

1.3 Results of Previous Workers.

Absorption spectra of the aromatic hydrocarbons have been measured in the visible region of the spectrum (1.22) (1.23), and in the ultra-violet (1.24). In general, absorption spectra of aromatic hydrocarbons consist of a

large number of prominent bands more or less equally spaced. The spacing interval between prominent bands in the vapour state is about 1300 cms^{-1} to 1400 cms^{-1}. Accompanying the banded spectrum is a background of continuous absorption which consists of two distinct regions separated by a region of transmission. The first absorption region is usually in the near ultra-violet. The second absorption region is at longer wavelengths and is much stronger than the first. For higher members of the series of aromatic hydrocarbons, the band spectrum becomes more diffuse and moves to longer wavelengths. The influence of the physical state on the absorption spectrum is a general band broadening and a shift to the red as the density of the medium increases. The relative positions of the components of the band system remain practically the same (1.23).

Figures 1 and 2 are absorption spectra of some hydrocarbons. FIGURE 1 shows the spectra of Anthracene (A), Naphthalene (B) and Benzene (C) in solutions of ethyl alcohol (1.25). FIGURE 2 is the absorption spectrum of crystalline anthracene (1.22) The wavelengths of maxima in the absorption spectrum of anthracene under various conditions are listed in TABLE 1. Anthracene has two main absorption bands in the ultra-violet region, at 3700 A.U. and at 2580 A.U. In the vapour state, there is a region of feeble transmission at about 3100 A.U. and there is an indication of another

such region, much less transparent, at 2600 A.U. (1.23).

The fluorescence spectra of the aromatic hydrocarbons, also become more diffuse and move toward longer wavelengths as the order of the series increases. Overlap between emission and absorption bands leads to modification of the fluorescence spectra due to reabsorption of fluorescent light. This is shown in FIGURE 3 which is the fluorescence spectrum of anthracene; in transmission through micro-crystals (A), in reflection from a 1 cm^3 crystal (B) and in transmission through a 1 cm^3 crystal (C) (1.26). The thickness of the crystal affects the structure and intensity of the transmitted fluorescence spectrum. With increasing thickness, the maxima of the curves shift slightly to longer wavelengths but, in the case of anthracene, the fluorescence spectrum shows no appreciable change for crystal thicknesses greater than 1 mm. (1.27). The wavelengths of principal maxima in the fluorescence spectrum of anthracene are given in TABLE 2.

Excitation spectra have not been reported in the literature to any great extent. Wright (1.16) and Driver (1.17) investigated the excitation spectrum of crystalline anthracene, and the wavelengths of maxima and minima obtained by them are listed in TABLE 3. Comparison with Table 1 shows that minima in the excitation spectrum correspond closely to maxima in the absorption spectrum. There is a

region of fine structure in the excitation spectra for exciting wavelengths between 1650 A.U. and 1510 A.U., and a prominent maximum at 2710 A.U. Typical excitation spectra for anthracene are shown in FIGURE 4 and in FIGURE 5. The surface condition of the crystal affects the intensity of the excitation spectra. The excitation spectrum of anthracene viewed in transmission after the front face of the crystal had been newly cleaved in air, showed no increase in intensity after cleavage. However on cleaving off the front face in vacuo, the intensity of the excitation spectrum increased after cleavage. Polishing the front face of the crystal had a quenching effect on the excitation spectrum and, in general, the excitation spectra of polished crystals were less intense than those of cleaved crystals. Scraping the front face of the crystal which is thought to enhance the surface escape of fluorescence (1.16), sharpened the maxima in the excitation spectrum. Spectra obtained from cleaved crystals were more intense when the (001) face was irradiated, than when the (010) face was irradiated.

The fine structure in the excitation spectrum between 1650 A.U. and 1510 A.U. was associated by Driver with the ionisation potential. Matsen (1.28) has calculated the ionisation potential of anthracene from theoretical considerations, and gives a value of 7.23 e.v. This is equivalent to radiation quanta of wavelength 1716 A.U.

However reference has been made to a much lower ionisation potential for solid anthracene by Tanaka (1.29), who suggested that photons of wavelength 2400 ± 200 A.U. should produce free electrons in anthracene crystals. It is possible that the peak in the excitation spectrum at 2710 A.U. is associated with the ionisation potential of anthracene and that the fine structure region, which coincides with the high energy maximum at 1600 A.U. in the hydrogen molecular spectrum, is characteristic of the light source and not of the anthracene itself. There is also evidence of a region of transmission in anthracene at 2600 A.U. (1.23), which enables the maximum at 2710 A.U. in the excitation spectrum to be explained by Wright's mechanism of "surface escape of fluorescence".

If, as is suggested, the ionisation potential of crystalline anthracene is in the neighbourhood of 5 e.v., irradiation of anthracene crystals by light of wavelength shorter than 2700 A.U., should make anthracene highly photoconducting. Experimental evidence for this has not been obtained although there is indication of an effect occurring at this wavelength. Carswell and Lyons (1.30) have drawn attention to the close correlation between the spectral dependence of the photoconduction of anthracene and the ultra-violet absorption spectrum. Maxima occur at identical wavelengths in the two curves, but at wave numbers above

37000 cm^{-1}, the resemblance between the photoconductance curve and the absorption spectrum apparently ceases. This is exactly equivalent to a wavelength of 2700 A.U., which is the wavelength of the large maximum reported by Driver in the excitation spectrum of anthracene.

In FIGURE 6, the reflection spectrum from the (001) face of an anthracene crystal is given (1.31). The percentage of monochromatic radiation reflected varies with the wavelength, but the variations are small and are of the order of 5%. The wavelengths of maximum reflection for an anthracene crystal are listed in TABLE 4 and comparison with Table 1 shows a correlation between wavelengths of maxima in the reflection and absorption spectra. These wavelengths correspond to minima in the excitation spectrum (cf. Table 3) within the limits of experimental accuracy, and an increase in reflection coefficient at wavelengths of maxima in the reflection spectrum would enhance the existing minima in the excitation spectrum.

The crystal structure of anthracene is monoclinic with two molecules per unit cell (1.32). Anthracene is birefringent and its optical properties vary with the orientation of the crystal to the incident light vector. The molecules are nearly flat and lie parallel to the bc plane, with similar stacking to graphite. The spacing between planes is 3.52 A.U. (1.11). The binding force between planes seems

to be stronger than between molecules in the same plane, as the most important natural face of the crystal is the (001) or (ab) face, which is also the cleavage plane. Anthracene cleaves in the (010) direction as well, though not as easily as in the (001) direction. There is evidence that energy transfer occurs more easily between molecules in adjoining planes than between molecules in the same plane.

1.4 Surface Effects, Defects and Impurities.

In the previous section it was shown that excitation spectra of anthracene crystals are sensitive to the condition of the crystal surface. For excitation by ultraviolet light in the fundamental absorption band, anthracene has an extinction depth of less than 1.4×10^{-4} cms and at 2850 A.U. the extinction depth is approx. 10^{-4} cms (1.33) Therefore most of the radiation incident on an anthracene crystal is absorbed by a thin layer of excited surface molecules. Anthracene reacts readily with oxygen to form an oxide of anthracene, anthraquinone, on the surface (1.34). In the presence of light of short wavelengths, anthracene forms a non-fluorescent layer of dianthracene (1.35); and anthracene also contains impurities in the crystal lattice which are difficult to remove. Fluorescence of anthracene may not in fact be a property of the pure substance at all, but may be due to impurities or defects in the crystal, or

to surface layers formed on the reaction of anthracene with its environment. This section will concern the fluorescence of crystalline phosphors.

The excitation spectra of Wright and Driver give some information concerning the nature of the surface layer in the case of anthracene. Curve C of Figure 4 was obtained by irradiating the 001 face of a 1 cm^3 anthracene crystal which had been exposed to the atmosphere but had been kept in the dark for a long period. It has a low fluorescence efficiency compared with a freshly cleaved crystal, which indicates a quenching mechanism. The spectrum C has maxima and minima at the same wavelengths as spectra A and B, which suggests that the exciting light is absorbed by anthracene molecules followed by radiationless quenching by impurity molecules at the surface. The impurity was thought to be the oxide of anthracene, anthraquinone (1.16).

Driver (1.17) found that the excitation spectra of cleaved crystals were more intense than similar spectra from polished crystals, and suggested that polishing caused an increased formation rate of the oxide on the surface, which quenched the fluorescence. Polishing diminishes the intensity of reflectance of anthracene by about the same amount at all wavelengths, but does not alter the structure of the reflection spectrum (1.31). However, there was a gradual increase in the intensity of the excitation spectrum

after cleaving the crystal in vacuo. This effect was absent if the crystal was cleaved in air. In the former case, if there were enough oxygen molecules in the vacuum to combine with the anthracene; the oxygen had no quenching action, but just the opposite. It was suggested that the slow increase in intensity was caused by the gradual self-annealing of the newly formed crystal surface.

The presence of oxygen has a striking effect on another photoelectric phenomenon, photoconduction; which is also a surface process (1.36). Photoconductivity in the surface layers of crystalline anthracene was found to increase over its vacuum level when measured in the presence of oxygen or air, but the vacuum level was reobtained after pumping the cell for a considerable period. The increased photoconductivity was attributed to oxidation of the surface in the presence of light or oxygen. The initial product, the oxide, was formed rapidly but was unstable in the dark; the final product, the peroxide, was formed much more slowly (1.37). Such a two stage process of photo-oxidation with the intermediate product being fluorescent, could explain the results of Wright and Driver. The fluorescent oxide formed immediately after cleavage in vacuo would enhance Driver's excitation spectrum, while the spectrum of low intensity reported by Wright would be due to the quenching action of the peroxide formed during the storage period.

Even though anthracene reacts readily with oxygen, the similarity of the absorption and emission bands of anthracene to those of its related aromatic hydrocarbons would indicate that the absorption and emission spectra are characteristic of the anthracene itself, rather than a surface layer of the oxide. In certain cases, some variable absorption bands in anthracene are due to small amounts of anthraquinone as impurity (1.38), and while it is sufficient for mixed crystals to contain only 0.01% to 0.001% by weight of impurities for practically all the fluorescence to occur from electronic levels of the impurity molecules (1.39), it is unlikely that the main absorption and emission bands of anthracene are due to a "characteristic" chemical impurity. It has been suggested that anthracene crystals fluoresce by virtue of traces of oxygen impurity combined with some of the molecules in the lattice (1.16). The relative fluorescent efficiencies of anthracene, naphthacene and pentacene for visible light at 20°C, are about 0.9, 0.002 and 0 respectively (1.40) and this suggestion would be largely verified if the affinity for oxygen of these substance were shown to decrease in the same proportion.

The fluorescence of very pure anthracene has been shown to be associated with defects in the crystal lattice (1.41). Defects such as unfilled vacancies and interstitial atoms, would cause distortion of the crystal lattice and would lead

to a number of energy levels near the levels of the perfect lattice. Weak variable lines in the absorption spectra correspond to transitions between such levels. A relation between the luminescence spectrum and the weak lines near the region of intrinsic absorption has been established for stilbene crystals (1.42). It would seem that fluorescence generally occurs at lattice defects or impurities and that excitons act as the energy transfer states between absorption and emission centres.

1.5 Purpose of Investigation

There were certain drawbacks in the method used by Driver to obtain excitation spectra. The dispersive element of the monochromator was not rotated continuously but had to be adjusted manually to the desired excitation wavelength. Three distinct measurements were then required to obtain the relative quantum efficiency of the sample at this wavelength; namely a value for the photomultiplier dark current, a value for the photocurrent corresponding to excitation of the sample and then a value for the photocurrent corresponding to excitation of the standard phosphor. Each of these readings required a separate rotation of the sample holder in the spectrograph itself. Similar readings were then required at selected wavelengths in the spectral range to obtain the excitation spectrum. In view of the

nature of the spectrum, a fine net of wavelengths is required to resolve the fine structure in the region of 1600 A.U. This increased the time involved in recording a spectrum and also increased the probability of change of the experimental conditions during the course of a run, which took about six hours. It was desirable to design a spectrograph which would speed up the measuring process, which would provide a continuous record of the spectrum and which would avoid movement of the sample holder during the course of a run. It was also desirable to improve the sensitivity of the instrument in order to verify the fine structure region reported by Driver.

The purpose of this investigation was accordingly, the construction of a vacuum spectrograph capable of automatically recording the excitation spectra of the aromatic hydrocarbons for electromagnetic radiation in the wavelength range from 5000 A.U. to 1500 A.U. The performance of the spectrograph was to be tested by repeating the measurements of Driver on anthracene crystals, and it was hoped to improve on some of the procedures involved in Driver's method. Then the excitation spectra of other aromatic hydrocarbons in the series benzene, naphthalene, anthracene, naphthacene and pentacene were to be obtained with a view to explaining the process of fluorescence, and energy transfer in these crystals. In conjunction with these measurements, the effect

on the excitation spectra of cleaving the crystals in a vacuum was to be investigated with particular regard to anthracene.

1.6 Outline of Method.

Excitation of the phosphor was by modulated monochromatic radiation from a vacuum monochromator using a hydrogen light source. The continuous molecular spectrum emitted by a glow discharge in hydrogen gas was split up into its wavelength components in the monochromator, a prism-mirror combination being the dispersive element. The wavelength of the radiation exciting the phosphor was varied over the spectral range by rotating the prism-mirror mounting. This was an automatic process using a synchronous motor operating from without the vacuum. The hydrogen discharge tube was driven by an A.C. power oscillator at a frequency of 200 Kc/sec. This caused the discharge tube to strike twice during each cycle of the oscillator so that the emitted light was modulated at twice the driving frequency of the oscillator.

The samples were placed at the exit slit of the monochromator, half the beam falling on a layer of sodium salicylate and the other half on the organic phosphor. Two DUMONT 6291 photomultipliers measured the fluorescent output, transmitted through the samples, as the wavelength

of the incident radiation was varied. The resulting photocurrents were amplified by R.F. amplifiers which were tuned to 400 Kc/sec. The outputs from the R.F. amplifiers were rectified and fed into separate D.C. logarithmic amplifiers. The signals from the logarithmic amplifiers were then passed to a difference amplifier, and the output was recorded on a variable response pen recorder. In this way the pen recorder registered a deflection proportional to the logarithm of the ratio of the fluorescent outputs of the two phosphors. As the wavelength of the exciting radiation changed, the deflection was recorded as a trace on the moving graph paper. The graph represented the logarithm of the ratio of the hydrocarbon fluorescence to the sodium salicylate fluorescence as the incident wavelength was varied, and as such was a direct reading of the absolute excitation spectrum of the organic phosphor. The detecting circuit is shown in block diagram form in FIGURE 7.

The modulated light method used here required tuned circuits in the detecting amplifiers. Large amplification is possible with A.C. circuits which are generally stable, and only the fluorescent signal and that portion of the noise spectrum falling within the bandwidth of the amplifiers is detected. Thus the use of turned circuit loads instead of purely resistive loads as would have been the case with a D.C. amplifying system, should reduce the level

of thermal noise and increase the signal to noise ratio of the instrument by limiting the D.C. component of the dark current.

Chapter 2

MODULATION

2.1 Conditions of Modulation.

The nature of light emitted by a discharge tube containing air at low pressure excited by a high frequency oscillator, was first investigated by Frey in 1936 (2.1). It was found that the light intensity oscillated at the exciting frequency of the discharge for frequencies as high as 10 Mc/sec. Frey calculated that the light emitted from the excited air atoms persisted after excitation for a period of approximately 5×10^{-8} sec., and that the illumination lagged behind the driving potential by a considerable fraction of a cycle at the higher frequencies.

Hamilton recently used a modulated light method in the measurement of photofluorescence decay times of organic phosphors (2.2.). Oscillation frequencies as high as 30 Mc/sec. were used. The method involved exciting the phosphor by light from an air discharge driven by a power oscillator, and measuring the relative degree of modulation of the exciting and fluorescent light. A photomultiplier tube detected the light given out by the phosphor. The pressure of air in the discharge tube was of the order of cms Hg. As the air pressure in the discharge tube was increased, the degree of modulation of the emitted light

increased but the intensity of the discharge decreased. The intensity decreased owing to the increased collisional quenching of the excited air molecules with increase in pressure. At the same time, the life time of the excited molecules was reduced causing an increase in the degree of modulation of the emitted light.

For modulation to occur, the variations in the intensity of the discharge should follow the oscillations of the exciting voltage. Since the process of light emission in a gas is due to electronic transitions of excited molecules to the ground state and to recombination of ionised states; the rates at which these relaxation and recombination processes occur, determines the degree of modulation at a particular frequency. If the reciprocal of the driving frequency of the discharge is appreciably less than the recombination time constant, then modulation of the light would be negligible. In the case of a gas having a number of excited states all with the same decay time, it is likely that with increasing excitation frequencies, the degree of modulation would decrease in an oscillatory fashion to zero at high frequencies. However, different energy states usually have different decay times, so that a small degree of modulation will occur even at high frequencies of excitation.

The present investigation is concerned with the application of modulation to radiation emitted from a hydrogen light source. The choice of driving frequency must be such that a high degree of modulation of the emitted light is obtained and this is dependent on the recombination and relaxation processes in excited molecular hydrogen.

2.2 Recombination Processes in Hydrogen Glow Discharges.

Glow discharges in air have been widely studied and it is probable that similar processes occur in hydrogen glow discharges under similar conditions of excitation. The cathode region is the main region of light emission in low pressure air discharges. It is also of interest in this investigation as the exciting radiation was light which had travelled down the length of the hydrogen discharge and had left the discharge tube through the cylindrical cathode. Therefore, it is likely that the spectrum is due to processes occurring in the region of the cathode.

At the cathode, electrons are liberated from the electrode due to bombardment by positive ions. The liberated electrons proceed back to the anode passing through the region of cathode glow and gaining energy in the process. It is only after the electrons begin to slow up after a number of ionizing collisions that the intense light emission occurs in the negative glow. In this region

where the energies are low there would be considerable recombination of electrons and positive ions, and there would also be a large concentration of excited molecules producing the emission spectrum in the visible and ultraviolet.

Recombination data give some information about these emission processes. The basic equation defining recombination is given by

$$\frac{dn}{dt} = -an^2$$

where "a" is the recombination coefficient and "n" is the concentration of positive or negative particles. Various types of recombination occur at different pressures and the value of the coefficient depends on the conditions under which the measurements were made. Loeb (2.3) has listed the various types of recombination process and the conditions under which they are likely to occur. At low pressures, either electronic or ionic volume recombination occurs and for hydrogen these two processes are equivalent. Here it is assumed that two particles of opposite sign do not combine unless they approach each other closer than a certain critical distance. Then recombination only occurs if a gas molecule is present to absorb the excess energy of collision. At low pressures, the mean free path becomes large compared to the critical distance of approach and "a"

becomes directly proportional to the pressure. TABLE 5 gives values for the volume recombination coefficients of oxygen, nitrogen, argon, hydrogen and air obtained by Luhr (2.4). The figures given in Table 5 are characteristic of volume recombination between ions and the low value for hydrogen indicates that ionic recombination occurs with less frequency than for the other gases reported. A value of 10^{-10} has been reported for the volume recombination coefficient of hydrogen in the particular case of a low pressure discharge (2.5). This and the low value of "a" reported by Luhr, shows that the amount of recombination between ions in a hydrogen discharge is small, and is insignificant in comparison with thermal excitation as the primary process of light emission.

The usually accepted relaxation time of the Lyman lines of hydrogen is 10^{-8} sec. (2.6). However Rayleigh (2.7) has reported that under certain conditions the time of relaxation was much longer than this and was of the order of 10^{-5} sec. In Rayleigh's experiment, the luminosity of hydrogen was examined for oscillation after it had been excited by an electrodeless discharge of a condenser and had been blown out of the electric field by its own expansion. No oscillations were observed. However, oscillations were detected if the hydrogen was replaced by nitrogen. The light examined was not part of the hydrogen

molecular spectrum and at the time of observation was out of the exciting field, so Rayleigh's result does not necessarily apply to glow discharges in hydrogen. However, it is evident that the after glow in hydrogen can exceed the mean life of the excited state in certain cases.

A relaxation time of 10^{-5} sec is equivalent to a period of electromagnetic radiation of frequency 100 Kc/sec. As the discharge strikes twice for every cycle of the alternating voltage, this would produce a modulation of approximately 25%. At higher frequencies, the degree of modulation would decrease until the driving frequency produces no variation in the output intensity of the discharge. This would then correspond to D.C. excitation.

2.3 Results.

The hydrogen discharge was initially excited at a frequency of 6 Mc/sec as it was hoped that the apparatus could later be adapted for decay time measurements on organic phosphors. At this frequency, no A.C. component of the hydrogen spectrum was detected at the exit slit of the monochromator. The D.C. component was observed. The driving frequency was then reduced to 200 Kc/sec and the A.C. component was detected. It would seem that although modulation frequencies of up to and possibly greater than 30 Mc/sec can be superimposed on an air discharge, there is

a much lower limit to the modulation frequency which can be applied to a hydrogen discharge.

FIGURE 8(A) shows the variation of the percentage modulation of light emitted from an air discharge, with pressure of air in the discharge tube in Cms Hg (2.8). Below an air pressure of 10 cms, the degree of modulation was found to decrease. Also reproduced in FIGURE 8(B) is the variation of the A.C. and D.C. components of the visible hydrogen spectrum with the pressure of hydrogen in the discharge tube. The intensities of the two curves in Figure 8(B) are not normalized. In contrast to air, both the A.C. and D.C. components of the hydrogen spectrum increased with decreasing hydrogen pressure. Maximum A.C. response which is equivalent to the maximum degree of modulation, occurred at 1 mm Hg pressure of the hydrogen in the discharge tube.

Chapter 3

APPARATUS

3.1 Introduction.

The vacuum monochromator and the power oscillator to be described in this Chapter were not built by the author but were originally used by A.S. Driver and T.D.S. Hamilton in the same Department. The monochromator which is shown in FIGURE 9, was modified for the present investigation. The original glass vacuum lines were changed to copper piping and an additional chamber was installed in the vacuum unit for mounting a synchronous motor. A new system of levers for rotating the dispersing element of the monochromator was introduced. The power oscillator for driving the discharge tube was used by Hamilton in the range 15 to 30 Mc/sec for the measurement of photofluorescent decay times of organic phosphors (2.8). It was retuned to 200 Kc/sec for this investigation.

3.2 The Monochromator.

The monochromator was a prism instrument of simple design and is shown in Figure 9. The dispersive element consisted of a prism with a concave aluminised mirror immediately behind it which collected the radiation travelling through the prism from the input slit, and

reflected it back through the prism onto the exit slit. The wavelength of radiation falling on the exit slit was varied by rotating the prism-mirror combination about its axis. For focus to be maintained, the optical path length for each wavelength passing through the prism should remain constant as the prism rotates. Accordingly, a thin prism of 5° refracting angle was used and this reduced the dispersion of the spectrum. However, the dispersion increased at shorter wavelengths which was an advantage for measurements in the ultra-violet region.

The prism-mirror combination (A) was mounted on a horizontal cantilever (B) which consisted of Dexion girder rigidly reinforced by brass plates (C) at both ends. The fixed end of the cantilever was attached to a steel base plate (D), while at the free end was mounted the turn-table (E) on which stood the prism and concave mirror as a unit. Light from a hydrogen discharge tube entered the monochromator through a hole (F) in the base plate. After passing through an entrance slit (G) consisting of a Hilger Type III variable slit mounted on a slide, the light travelled the length of the cantilever to the prism-mirror combination. Here it was refracted by passage through the prism, reflected by the mirror, and after a further refraction, the deviated beam travelled back to the base plate. The emerging beam travelled down a length of copper piping (H) soldered into

a hole in the base plate. At the end of the copper piping was situated the exit slit of the monochromator (cf. Figure 13). The width of the exit slit could be adjusted but its distance from the axis of the prism was fixed. Focussing was achieved by moving the input slit, and obeys the relation $\frac{1}{u} + \frac{1}{v} = \frac{1}{f}$

where u = distance from entrance slit to mirror

v = distance from exit slit to mirror

f = focal length of concave mirror.

The vacuum chamber (I) was formed by a length of steel water piping of approximately 5" internal diameter, mounted on a trolley. This was positioned to enclose the cantilever and to make contact with the base plate by means of a flange. An O ring seal ensured tight contact under vacuum. The exhaust line entered the vacuum chamber through a hole (J) in the base plate. Access to the input slit and the prism-mirror unit was obtained by unbolting the flange and sliding back the pipe on its special trolley.

For convenient mounting of a synchronous motor, a small chamber (K) was introduced between the removable housing and the base plate. This formed an additional part to the main chamber and was made of similar piping. It contained a Wilson Seal (L) screwed into the casing and welded in position for tightness under vacuum. With the driving mechanism in position, the chamber remained permanently

bolted to the base plate. In this way, the main vacuum chamber could be opened without each time disturbing the calibration of the revolution counter attached to the synchronous motor.

The prism, and the window separating the discharge tube from the monochromator were made of calcium fluoride which transmits useful radiation down to 1250 A.U. The mirror reflecting the radiation had an aluminium surface, which has a reflectivity of 90% down to 2400 A.U. but falls off to 30% at 1200 A.U. Its reflectivity does not suffer seriously by ageing (3.1). The monochromator was evacuated to a pressure of less than 10^{-5} mm Hg during the course of a run, so there was little absorption of light by residual gases in the instrument itself. As the molecular spectrum of hydrogen consists of a continuum down to 1700 A.U. and a many lined spectrum at shorter wavelengths (3.2), the monochromator should transmit a useful intensity of light down to 1200 A.U. However, the dispersion of the prism is non-linear, and a different range of wavelengths is passed by the exit slit in different regions of the spectrum. TABLE 6 gives the dispersion of the monochromator at various wavelengths and also the range of wavelengths passed by a slit of width 0.10 mm at the same wavelength.

The cantilever of the monochromator with the main vacuum chamber removed is shown in PLATE 1. The prism-mirror

combination is visible, as is the chamber with the synchronous motor in position.

3.3 Prism-Mirror Housing and Rotation Mechanism

FIGURE 10A shows the Rotation Mechanism and FIGURE 10B shows the Prism-Mirror Unit. The turntable supporting the prism (A) and mirror (B) consisted of two circular brass discs (C), the one positioned just above the other by three spring loaded screws. The top disc which supported the prism and mirror was levelled using these screws. Attached to the centre of the bottom disc was a steel shaft (D), which formed the axis of rotation of the prism-mirror unit. The shaft fitted into a cone-shaped housing (E) which was clamped to the cantilever (F). The unit was rotated in this housing by means of a brass rod (G) attached to the shaft extending below the cone-shaped housing. The rod (G) was rectangular in cross-section and acted as a lever which could be moved in the horizontal plane by a probe pushing at the other end of the rod.

Movement was achieved by advancing the flat tip (H) of a micrometer screw gauge (I) against the spherical surface of a ball bearing soldered to the rod. Continuous contact between the spherical and flat surfaces was maintained by springs (J). One spring was at the end of the rod and was attached to the clamp (K) holding the screw gauge in place.

The other spring was half-way down the rod and was connected to the arm of a support for the rod. The support consisted of a flat brass strip fitted below the cantilever (cf. Figure 9), and the rod (G) rested on this support by means of a ball-bearing to reduce friction. As the dispersion of the instrument was relatively low, the angle of rotation required to sweep the ultra-violet spectrum across the exit slit was small also. Rotation of the prism-mirror combination through an angle of less than 2^{o} was sufficient to change the wavelength at the exit slit from 6000 A.U. to 1300 A.U. The distance travelled by the end of the rod to produce this rotation was less than 1.35 cm. The corresponding drift of the point of contact of the ball-bearing on the screw-gauge head as the rod was displaced, was of the order of 0.03 cms, and was easily accommodated by the screw-gauge head.

The system required precise positioning of the components of the rotation mechanism. When the chamber (L) housing the screw-gauge was clamped to the base plate, the screw-gauge head made contact with the ball bearing on the side of the rod (G). The screw-gauge (I) fitted through a pipe (M) in the side of the chamber and was under vacuum when the chamber was evacuated. The screw-gauge head was rotated from outside the vacuum by a small diameter rod (N) passing through a Wilson seal. This allowed translational

as well as rotational movement down the axis of the rod. The rod (N) was connected to the drive of a synchronous motor and a sliding sleeve device took up the inward motion of the rod. A revolution counter was coupled to the driving shaft of the synchronous motor and one revolution of the screw-gauge head was accomplished every two minutes.

The rotation mechanism was required to reproduce exactly the spectral lines corresponding to a particular setting of the revolution counter. This depends largely on the screw gauge. Being a high precision instrument, irregularities in its thread were negligible. The surface of the screw-gauge head making contact with the ball bearing was also accurately planar. Backlash was avoided by rotating continuously in the same direction. A feature of the mechanism was the small number of moving parts needed for rotation.

3.4 The Vacuum System

A diagram of the vacuum system is given in FIGURE 11. A dynamic pumping system was employed with a Leybold Type 03 Oil Diffusion Pump backed by an Edwards "Speedivac" Rotary Pump. When the system was vacuum tight, the Rotary Pump attained a pressure of 5×10^{-3} mm Hg in ten minutes. Using Apiezon B oil, the diffusion pump attained a pressure of 5×10^{-5} mm Hg in the apparatus after a further

30 minutes pumping, although this period was influenced by the rate of outgassing of the apparatus. When the system had reached a pressure of less than 10^{-4} mm Hg, the discharge tube was sealed off from the rest of the system and was filled with hydrogen. During a set of readings, the monochromator was continuously evacuated by the diffusion pump backed by the rotary pump.

After a set of readings, it was possible to keep the hydrogen in the discharge tube for periods up to four hours without the need for continuous pumping of the monochromator. For longer storage periods, there was the danger of small leaks in the apparatus causing a pressure difference to develop across the fluorite window which separated the discharge tube from the monochromator. Large pressure differences might crack the window. The apparatus was generally left under vacuum with the discharge tube open to the rest of the system when not in use. Joints in the system were made vacuum tight by means of O rings greased with Apiezon M grease. For glass to copper joints, vacuum wax was used successfully, especially if the joint was coated with shellac while the apparatus was under vacuum. The pressure in the apparatus was measured by a Pirani Vacuum Gauge with an Ionization Gauge for pressures below 10^{-3} mm Hg. The gauges formed a Pye "Cathodion" Combined Pirani Ionization Gauge unit.

3.5 The Radiation Source.

The discharge tube was cylindrical in shape, water cooled and was made of quartz glass by the Thermal Syndicate. It is shown in Figure 11. Radiation passed down the axis of the discharge tube, through the cylindrical cathode, through a fluorite window and into the monochromator. The cathode end of the discharge tube was fitted with a brass flange similar to one on the inlet pipe to the monochromator. The axis of the discharge tube was lined up with the prism-mirror combination, movement being taken up by a metal bellows in the lead to the monochromator. When aligned, the two brass flanges were clamped together, a rubber O ring between the flanges forming the vacuum seal.

The vacuum line entered the discharge tube behind the anode. Mounted next to the vacuum line was a palladium rod connected to the discharge tube by a graded glass to quartz joint. Hydrogen was introduced into the discharge tube by first evacuating it to a pressure less than 10^{-4} mm Hg, and sealing it off from the rest of the system. Then, cooling the joint of the palladium metal to the discharge tube with moist cotton wool, the palladium leak was heated with a small hydrogen flame until a volume of hydrogen equivalent to 2 mm Hg pressure had diffused through. The pressure of gas in the discharge tube relative to the rest of the apparatus was read off from a glass manometer

containing Apiezon B oil fitted across the tap sealing off the discharge tube from the rest of the system.

3.6 The Voltage Source.

The large alternating potential required to drive the hydrogen discharge was provided by a power oscillator. With a hydrogen pressure of 4 mm Hg, a R.M.S. potential of 1800 volts applied across the electrodes started the discharge. There was no distinct striking voltage as the R.F. potential was increased. The oscillator worked off two power supplies and its circuit diagram is given in FIGURE 12.

1. The Oscillator. The frequency of oscillation was controlled by a 100 Kc/sec crystal in the grid of the first stage. The second and third stages were amplifiers tuned to the second harmonic of the first stage frequency. The 200 Kc/sec signal was applied to the grid of the fourth stage - a Class C power amplifier, and the discharge tube was tapped from the coil of the tank circuit of this last output stage, to earth.

2. Power Supply Nos. 1. This provided a stabilised D.C. voltage to the plates of the first three stages, and to the screen grid of the fourth stage of the power oscillator. The circuit is given by Elmore and Sands and delivers a current up to 225 ma at 450 volts (3.3.).

3. Power Supply Nos. 2. This supplied a voltage ranging from 0 to 2000 to the plate of the fourth stage of the oscillator. A variac control on the mains input enabled the voltage to be varied over this range, and the mains supply was governed by a water pressure switch in the cooling system of the discharge tube. The circuit is given by Hamilton (2.8).

3.7 The Detecting System.

1. Sample Chamber. The crystals were mounted in vacuo in a chamber which was fitted to the exit tube of the monochromator (FIGURE 13). The exit tube (A) was a partial support for the chamber and also served as the vacuum line. The chamber (B) was a cylinder open at one end, of diameter 16 cms and length 5 cms. The open end of the chamber was sealed off by a circular base plate (C). Cut into the plate were two rectangular apertures which held the light guides (D). When the plate was in position, half of the beam emerging from the exit slit fell on the upper light guide, and the other half fell on the lower light guide. The crystal phosphors were mounted in front of the light guides immediately behind the exit slit. In this way, splitting up the exciting radiation before it struck the crystals was avoided; and as light from the same beam fell on both samples, changes in source radiation intensity, and

absorption in the spectrograph affected both channels to an equal extent. The light guides were approximately 1 cm x 1 cm in cross-section and were made of solid perspex. Their surfaces were silvered by the usual cathodic sputtering technique and they were cemented into the base plate with Araldite Adhesive.

2. Photomultipliers. The fluorescent light was detected and amplified by photomultipliers mounted behind the light guides. The close proximity of the light channels necessitated the use of $1\frac{1}{2}$" diameter phototubes. Two DUMONT type 6291 tubes of high sensitivity were used. These have a spectral response from 3200 A.U. to 5600 A.U. and a rated current amplification of 10^6 at a cathode potential of -2000 volts. The photomultipliers were mounted in separate, light tight, housings which fitted into retaining rings on the base plate. The radiation from the crystals travelled down the light guides onto the photocathodes of the photomultipliers. The anode current from each unit developed a voltage across an impedance consisting of a parallel resonance circuit tuned to 400 Kc/sec. The voltage was fed to the next stage by means of coaxial cable.

3. R.F. Amplifiers. The circuit diagram of the R.F. amplifiers is shown in FIGURE 14(a). They consist of two transformer-coupled pentodes, the transformer of the last stage of each amplifier being used as an isolating

transformer, to enable the common line of the succeeding stages to be at 180 volts negative. The gain and bandwidth of each amplifier was approximately 80 dB and 6 Kc/sec respectively. A semiconductor diode rectified the amplified signal and fed it to the next stage which was a D.C. logarithmic amplifier.

4. D.C. Logarithmic Amplifiers. The circuit diagram is given in FIGURE 14(b) and an analysis of its action is given in (3.4) and in the Appendix. The amplifier consisted of a double triode and differences in characteristics between the tubes were compensated for by variable potentiometers in the circuit. The output was adjusted to follow the equation

$$E_o = 9{\cdot}00 - 2 \log_{10} E_i \text{ volts.}$$

with an accuracy of better than 2% for positive inputs from 5 to 500 volts. The response of the logarithmic amplifier is given in FIGURE 15. The adjustment was achieved by setting R2 to give an output of 9 volts for zero input voltage. Then with 50 volts input, R1, was adjusted for an output of 5.6 volts and finally, R3 was adjusted to give an output as near as possible to 7 volts for an input of 10 volts. R1 and R2 usually required frequent fine adjustment but R3 did not normally require it. For logarithmic response, the amplifier needed a high impedance load. In this case, the next stage was a difference

amplifier of high input impedance so a matching stage was not required.

5. Difference Amplifier. The circuit diagram of the difference amplifier is given in FIGURE 14(c). The output which was proportional to the difference of the two signals impressed on the grids was taken across the plates of the amplifier. The positive H.T. terminal of the amplifier was earthed to enable the average output voltage to be as near earth potential as possible. A 7.5 volt cell coupled in parallel with a potentiometer in the output line to the pen recorder, enabled the steady state output voltage of the difference amplifier to be backed off so that equal input signals gave a zero output signal. A potentiometer in the cathode circuit of one of the triodes of the difference amplifier allowed further small zeroing adjustments to be made.

6. Pen Recorder. This was a VARICORD Model 42A pen recorder. Its response was variable and could be expressed either as a linear function of the input voltage, a logarithmic function of the input voltage, or some relation between the two. Its sensitivity could be adjusted to give a full-scale deflection ranging from 5 mv to 10 volts. Full scale deflection was achieved in about one second and the chart speed was 0.85 inches per minute.

Chapter 4

EXPERIMENTAL

4.1 Introduction.

Two frequencies of modulation of the exciting radiation were tried. For modulation at 12.85 Mc/sec, no modulated signal corresponding to the hydrogen spectrum was detected. At the lower frequency of 400 Kc/sec, modulated signals were recorded. For this reason, the description of apparatus given in Chapter 3 describes the experimental set up at the lower frequency. As electromagnetic radiation is strongly absorbed by air below 1900 A.U., a vacuum of less than 10^{-5} mm Hg in the monochromator was essential. The experimental procedure to obtain this has been described in Section 3.4 and will not be dealt with in this Chapter. PLATE 2 is a photograph of the apparatus.

4.2 Excitation at 6.425 Mc/sec.

The power oscillator (Figure 12) was tuned to a frequency of 6.425 Mc/sec. Two methods of coupling the discharge tube to the oscillator were tried. Transformer coupling was unsatisfactory because of the detuning effect on the oscillation frequency introduced by the reflected impedance from the secondary to the primary coil. A shunt fed method was preferred, and the detuning effect

of the discharge tube was compensated for by tapping off the lead to the discharge tube at a suitable point on the coil of the last stage of the oscillator. To reduce the capacitance of the discharge tube circuit to a minimum, the coaxial lead from the oscillator was made as short as possible. Radiation loss from the discharge tube and from the oscillator was appreciable and caused spurious voltages on the detecting circuitry. This was largely eliminated by decoupling all leads to the oscillator, by shielding the oscillator and by wrapping the discharge tube with aluminium foil. The discharge tube was effectively a continuation of the coaxial cable and the aluminium foil acted as the return path to earth of the current of the discharge.

The optical system was focussed by removing the discharge tube and replacing it with a HANOVIA mercury lamp, as the hydrogen tube could only be used with the apparatus under vacuum. A microscope was focussed on the exit slit of the monochromator. The exit slit was then removed to enlarge the field of view. The length of the input slit was set in the vertical plane and its position was adjusted relative to the mirror to give clear focus of the mercury spectrum in the plane of the exit slit. The prism turn-table was levelled to ensure that the spectrum remained in the same horizontal plane as the turn-table was rotated. The discharge tube was then remounted, and by shining a

bright light down its axis, was aligned with the prism-mirror combination so that uniform illumination of the input slit was visible at the exit. The exit slit was then replaced parallel to the image of the input slit.

The detecting equipment consisted of an R.C.A. 6342 photomultiplier tube and a two stage pentode amplifier tuned to 12.85 Mc/sec. The current amplification of the R.C.A. 6342 phototube was rated at 12×10^4 and the tuned amplifier could detect a signal of 1 mv applied to its input terminals. The gain of the amplifier was 800. The voltage developed across the photomultiplier load resistor was amplified, rectified with a diode and measured by a Simpson Model 260 Multimeter connected across a resistor in the rectifying circuit.

An attempt was made to detect the visible hydrogen spectrum. A perspex disc was placed over the exit slit of the monochromator; and the window of the photomultiplier tube was placed immediately behind it. The monochromator was evacuated and the discharge tube was filled with hydrogen at 5 mm pressure. The discharge was started and the visible part of the spectrum was moved across the exit slit. No deflection corresponding to spectral lines was obtained on the Simpson meter. The 6342 photomultiplier was then replaced by an R.C.A. 5819 tube, but no modulated signal was detected. The photomultipliers were then tested for

D.C. response using a Beckman Spectrometer as light source. The circuit consisted of the photomultiplier with the same dynode resistors and base as before, a potentiometer, and a Tinsley Spot Galvanometer connected across the potentiometer. Both photomultipliers were found to be sensitive to the visible region of the spectrum.

An attempt was then made to detect the D.C. component of the hydrogen spectrum emerging from the monochromator, using the above method. An average deflection of 1 cm corresponding to the visible spectrum registered on the Tinsley galvanometer but no individual lines were resolved. The sensitivity of the galvanometer was 240 mm/microamp which indicates that the anode photocurrent was 0.04 microamp. This is of similar order to 0.12 microamps obtained by Driver when recording the hydrogen spectrum with sodium salicylate as sensitizer. The photomultiplier load was 750 ohms and allowing for an associated capacitance of 20 micro-microfarads between the anode and other electrodes, the impedance presented to the photomultiplier at 12.85 Mc/sec was 350 ohms. Therefore, the D.C. voltage developed across the photomultiplier load was of the order of 0.01 mv. It was possible that the modulated component of the signal was smaller than the D.C. component and therefore below the sensitivity of the tuned amplifier, which was 1 mv.

For this reason, an attempt was made to detect a much smaller A.C. signal. The tuned amplifier was replaced by an R206 Radio Receiver fitted with an extra i.f. stage and capable of detecting an input voltage of 10 microvolts. The radio receiver was tuned to a frequency of 12.85 Mc/sec, and the signal from the receiver was investigated by rectifying the output from the final i.f. stage and measuring the voltage drop across a resistor in the rectifying circuit with a Simpson meter. It was found that radiated pick-up in the receiver obscured any modulated signal that was present. The noise voltage was appreciable as the detecting system was operating at a harmonic of the exciting oscillator.

A more sensitive method of detection was then tried whereby the modulated signal from the photomultiplier was mixed with a signal from an R.F. oscillator, and the radio receiver was used to amplify the beat frequency. The beat frequency was chosen so that it bore no relation to the frequency of the discharge. The mixer circuit which employed a semiconductor diode, was mounted in the photomultiplier casing for adequate shielding. The discharge was started and the visible hydrogen spectrum was arranged to fall on the exit slit of the monochromator. With the Radio Receiver tuned to 1 Mc/sec, the signal generator frequency was varied about 13.85 Mc/sec. The visible

spectrum was then moved across the exit slit of the monochromator, but no voltage variation registered on the Simpson meter measuring the output of the radio receiver.

The conclusion was reached that, at the driving frequency of 12.85 Mc/sec, the degree of modulation of the hydrogen radiation was too small to be detectable by the A.C. detecting unit. At this stage of the experiment, it was thought that the degree of modulation would increase with increasing pressure of the hydrogen in the discharge tube, as is the case in an air discharge. So the discharge was never run at low hydrogen pressures which were later found to give the best degree of modulation.

4.3 Excitation at 200 Kc/sec.

In view of the negative result obtained for a modulation frequency of 12.85 Mc/sec, the driving frequency of the hydrogen discharge was reduced to 200 Kc/sec. This would increase the degree of modulation, and is more within the range of frequencies for which modulation of light from a hydrogen discharge should occur (Section 2.2). The frequency of 200 Kc/sec was chosen for convenience of detection. The fluorescent signal would then be modulated at a frequency of 400 Kc/sec, which enabled the use of standard I.F. transformers in the amplifying stage of the detecting unit.

The oscillator was adapted to operate at 200 Kc/sec. The amplifiers described in Section 3.7 were built and tested. During a bench test, it was verified that input signals to the R.F. amplifiers greater than ten microvolts were detectable, and that the signals could be reproduced with reasonable accuracy on the pen recorder. Sluggishness in the response of the pen recorder and voltage drift of the logarithmic amplifier was encountered. The sluggishness was due to A.C. hum pick-up in the recorder and was eliminated by reversing the polarity of the mains supply. The voltage drift was reduced to negligible proportions by allowing the D.C. amplifiers to warm up for a number of hours before commencing readings.

A preliminary investigation was made of the visible hydrogen spectrum to detect the D.C. component of the light. A DUMONT 6291 photomultiplier was used in conjunction with a potentiometer and the Tinsley galvanometer. The optical system was aligned and the crystal chamber was mounted in position on the monochromator, the exit slit having been removed to enable the complete visible spectrum to fall on the light guides. The hydrogen discharge was started and a D.C. component of the light was detected in both channels. The deflections registered by the galvanometer using first the upper light guide and then the lower light guide, were compared; and the prism turn-table was

levelled to give approximately equal illumination of both channels.

An attempt was then made to record the modulated signal. One of the R.F. amplifiers was tuned to the 2nd Harmonic of the Oscillator by connecting an aerial to the amplifier input and tuning to the radiated signal of the oscillator, the rectified output of the amplifier being measured with a Simpson meter. The amplifier was then connected to the DUMONT 6291 photomultiplier and on sweeping the visible spectrum across the light guides, modulated signals were detected in both channels.

The exit slit was replaced and the complete detecting circuit was coupled to the photomultiplier. (cf. Figure 7). Only one channel was used, the input grid of the other R.F. amplifier being grounded. The sensitivity of the pen recorder was adjusted to give full scale deflection for an input signal to the one R.F. amplifier of 20 microvolts. At the same time, the backing potential in the output lead from the difference amplifier, was set to give zero output from the difference amplifier for zero input voltages.

On increasing the E.H.T. to the phototube above 1000 volts, a deflection was observed on the pen recorder. Increasing the E.H.T. still further caused the trace to become very unstable. This was thought to be due to thermal noise in the photomultiplier load resistor, which,

for a 1 Megohm resistor in a circuit of bandwidth 6 Kilocycles at room temperature, is of the order of 10 microvolts. Accordingly the 1 Megohm resistor was replaced by a parallel resonance circuit tuned to 400 Kc/sec. This reduced the noise level but not the instability, and the noise level was still found to increase with increasing dynode voltages to values exceeding 10 microvolts. Reasons for the instability were investigated. Sand-papering and cleaning the pins, and socket holes of the photomultiplier base had no effect. The possibility of breakdown between the photomultiplier and the metal walls of the photomultiplier housing was minimised by inserting strips of film in the air gap as an insulating medium. The instability remained, and necessitated a maximum applied potential to the phototube of 1000 volts, which was below the rated maximum of 2100 volts.

Under these conditions, a reproducible trace was obtained on the pen recorder corresponding to the visible region of the spectrum. On sensitizing the surface of the upper light guide with a thin evaporated layer of sodium salicylate, a graph was obtained which showed two additional peaks in the ultra-violet region of the hydrogen spectrum. These are thought to correspond to the two peaks of high intensity previously reported in the line spectrum of hydrogen at 1200 A.U. and 1600 A.U. (4.1). The hydrogen

spectrum of Driver gives only one peak in the ultra-violet region, at 1500 A.U. (1.17). All the hydrogen spectra recorded showed two peaks in the ultra-violet region and a large extended peak in the visible region. Except for a general increase in the intensity of the spectrum towards longer wavelengths, there were no other reproducible features of the graphs obtained for the hydrogen spectra. Two typical traces of the hydrogen spectrum are given in FIGURE 16.

An anthracene crystal was then attached to the surface of the lower light guide, and its fluorescence was examined with the detecting circuit described above. In this case the grid of the R.F. amplifier in the sodium salicylate channel was grounded. As the exciting wavelength varied, the graph traced out by the pen recorder remained constant except for a deflection in the visible region of the spectrum. The difference between the anthracene sensitized graph and the sodium salicylate sensitized graph was the disappearance of the two peaks in the ultra-violet and a sharpening of the peak in the visible region. On increasing the E.H.T. to the photomultiplier above 1000 volts, the average deflection registered by the recorder increased, and the trace became progressively more unstable. This effect remained on bypassing the logarithmic and difference amplifiers, and connecting the output of the R.F. amplifier straight to the pen recorder.

With the detecting circuit connected to record the relative excitation spectrum, the graph traced out by the pen recorder showed no variation in the ultra-violet region when the two photomultiplier E.H.T.s were set to give a stable zero level of the trace. When the E.H.T. to the photomultipliers was increased, the instability of the trace increased and no reproducible features of the excitation spectrum emerged above the noise level.

Chapter 5

CONCLUSION

The results show that the vacuum spectrograph using a modulated hydrogen light source, can resolve and automatically record certain features of the hydrogen spectrum at modulation frequencies of 400 Kilocycles/second. However, the method of A.C. detection in its present form is not capable of resolving excitation spectra. This is due to the high noise level which is developed by the photomultiplier at large dynode voltages, and which is of the same order of magnitude as the fluorescent signal to be detected. At the low voltages required to reduce the dark current of the photomultiplier to a stable value, the fluorescent signals did not appear above the noise level.

Noise in photomultiplier tubes has been analysed by Engstrom (5.1). For low levels of light flux, there is unavoidable noise due to the random incidence of fluorescence photons which produce current fluctuations at the photocathode that are amplified by the tube. Associated with this, there is a dark current due to electrons emitted thermionically from the photocathode and dynodes, which is variably multiplied by the secondary emission gains of the dynode stages. In alternating current measurements with a modulated light source, the ultimate limitation to signal

detection is the thermionic emission from the photocathode. The r.m.s. value of the fluctuating output current caused by thermionic emission can be derived from the equation

$$\left(I^2_{Ave}\right)^{\frac{1}{2}} = G(2ei\Delta f)^{\frac{1}{2}}$$

where G = gain of photomultiplier

e = electronic charge

i = thermionic emission current from photocathode

Δf = bandwidth of receiving unit.

This equation neglects noise associated with thermionic emission from the dynodes, and that associated with the random process of secondary electron emission, both of which would increase the noise level. Assuming a typical value of 10^{-14} ampere for the thermionic emission from the photocathode at room temperature; the r.m.s. value of the fluctuating output current corresponding to a bandwidth of 6 Kilocycles and a gain of 10^6, is 0.004 microamperes. The impedance at resonance of the tuned photomultiplier load was of the order of 10 K ohms, and therefore the input signal to the R.F. amplifier was approximately 40 micro-volts, as observed. Since the current due to thermionic emission is amplified through the tube in the same way as the signal photocurrent, the noise level increased as the gain of the tube was increased. These values may be compared with

those obtained by Platt (5.2) when investigating the hydrogen spectrum using a sodium salicylate-sensitized R.C.A. 6342 photomultiplier and a D.C. method of excitation. The dark current was 0.01 microampere and the signal to noise ratio at 180^{0} A.U. was 30, with 1.3 Kilovolts across the tube.

If the modulated light method is to be developed as an alternative to the D.C. method, the signal to noise ratio of the detecting unit must be improved. Background currents should be limited, and in order to reduce ionization effects in the photomultiplier, the potential difference between subsequent dynodes should be limited to 100 volts. The signal to noise ratio could be enlarged by reducing the bandwidth of the amplifying system, as this would considerably reduce the noise level. Difficulties would have to be overcome in matching the frequency of the detecting amplifier to the oscillator frequency, and frequency drifts would have to be eliminated. Thermionic emission would be reduced by cooling the photomultiplier tube, and a photomultiplier refrigerator using liquid nitrogen as a refrigerant has been described (5.3). Refrigerating the photomultiplier lowers the noise level by about one decade of equivalent light intensity for an 80^{o}C drop in temperature (5.4). In addition, sensitivity would be improved by increasing the intensity and the degree of modulation of

the hydrogen discharge; and by using better reflecting surfaces, e.g. palladium, in the monochromator for reflection in the ultra-violet. However, the amount of significant improvement possible in this direction is small. It is probably simpler to use an unmodulated light source with D.C. detection.

Arising out of this work, it is suggested that the modulation of light from a hydrogen discharge be further investigated; and that a comparison of the A.C. components of light from a hydrogen discharge and an air discharge at the same modulation frequency be undertaken. Further, that the automatic recording spectrograph be used to obtain the excitation spectra of the aromatic hydrocarbons by D.C. detection. As well as cleaving the crystals in vacuo, it would be interesting to cleave in other gases in order to clarify the role of oxygen in fluorescence. The specimen chamber could be adapted to allow for the introduction of gases. In addition, if electrodes were introduced into the specimen chamber, photoconduction measurements could be made in conjunction with excitation measurements.

APPENDIX

Analysis of Action of the Logarithmic Amplifier.

The plate current of a thermionic triode can be given by

$$i_p = K_1(e_g + e_{p/\mu})^a \quad (1)$$

The grid current near region of zero grid voltage is

$$i_g = i_{go} \exp(^{e_g}/_{K_2}) \quad (2)$$

$$\therefore \quad e_g = K_2' \log_{10} i_g - K_2' \log_{10} i_{go} \quad (3)$$

Combining (1) and (3)

$$i_p = K_1(K_2' \log_{10} i_g - K_2' \log_{10} i_{go} + e_{p/\mu})^a \quad (4)$$

Therefore $$e_p = \mu\left[\left(\frac{i_p}{K_1}\right)^{1/a} - K_2' \log_{10}\left(\frac{i_g}{i_{go}}\right)\right] \quad (5)$$

R_1 selects a fraction "b" of input voltage

$$i_g = (bE_i - E_g)/R_g' \quad (6)$$

Substitute (6) into (5)

$$e_p = \mu\left\{\left(\frac{i_p}{K_1}\right)^{1/a} - K_2' \log_{10}\left[(bE_i - E_g)/i_{go}R_g'\right]\right\} \quad (7)$$

$$= C - K \log_{10}(E_i - {E_g}/{b})$$

where $$C = \mu\left[\left(\frac{i_p}{K_1}\right)^{1/a} - K_2' \log_{10}\left(\frac{b}{i_{go}R_g'}\right)\right]$$

and $$K = \mu K_2'$$

If $E_i \gg \mu K_2'$ then eq^n (7) becomes

$$e_p = C - K \log_{10} E_i$$

Significance of Symbols.

i_p = plate current

K_1 = constant depending on tube geometry

e_p = plate voltage

e_g = grid voltage

μ = amplification factor

a = constant = $^2/_3$

i_g = grid current

i_{go} = grid current for zero grid voltage

K_2 = a function of cathode temperature

K_2' = 2.306 K_2

E_g = grid to cathode voltage due to contact potential

E_i = input voltage

R_g' = effective series grid resistance

BIBLIOGRAPHY

1.1	Bowen E.J.	1942 The Chemical Aspects of Light. Clarendon Press.
1.2	Birks J.B. and Wright G.T.	1954 Proc. Phys. Soc. B67 417.
1.3	Pringsheim P.	1946 Fluorescence and Phosphorescence Interscience Publishers.
1.4	Stevens B. and Hutton E.	1959 Reprint from what? Chemistry Dept., Sheffield University.
1.5	Birks J.B.	1954 Phys. Rev. 94 6.
1.6	Sidman J.W. and McClure D.S.	1956 J. Chem. Phys. 24 4 757.
1.7	Kallman H. and Furst M.	a)1950 Phys. Rev. 79 857. b)1954 Phys. Rev. 94 3.
1.8	Bowen E.J. and Lawley P.D.	1949 Nature 164 572.
1.9	Lipsky S and Burton M.	1959 J. Chem. Phys. 31 5 1221.
1.10	Wright G.T.	1955 Proc. Phys. Soc. 68B 10 701.
1.11	Simpson O.	1957 Proc. Roy. Soc. A238 1214.
1.12	Choudhury N.K. and Ganguly S.C.	1960 Proc. Roy. Soc. A259 1298.
1.13	Clarke H.B., Northrop D.C. and Simpson O.	1962 Proc. Phys. Soc. 79.
1.14	Sidman J.W.	1956 Phys. Rev. 102 96.
1.15	Dewar M.J.S. and Longuet Higgins H.C.	1954 Proc. Phys. Soc. A67 417.
1.16	Wright G.T.	1955 Phys. Rev. 100 2 587.
1.17	Driver A.S.	1959 M.Sc. Thesis Rhodes University.
1.18	Watanabe K. and Inn E.C.Y.	1953 J. Opt. Soc. Am. 43 32.

1.19	Slavin W., Mooney R.W. and Palumbo D.T.	1961 J. Opt. Soc. Am. 51 93.
1.20	Hammann J.F.	1958 Z. f. Angew. Phys. 10 187.
1.21	Johnson P.D.	1961 J. Opt. Soc. Am. 51 11.
1.22	Kortum and Finckh	1942 Z. Phys. Chem. B52 263.
1.23	Seshan P.K.	1936 Proc. Ind. Acad. Sci. A3 148.
1.24	Klevens H.B. and Platt J.R.	1949 J. Chem. Phys. 17 5.
1.25	Mayneord W.V. and Roe E.M.F.	1935 Proc. Roy. Soc. A 152.
1.26	Cameron A.	1954 M.Sc. Thesis. Rhodes University
1.27	Little W.A.	1954 M.Sc. Thesis. Rhodes University
1.28	Matsen F.A.	1956 J. Chem. Phys. 24 602.
1.29	Tanaka J.	Reprint. Rhodes University.
1.30	Carswell D.J. and Lyons L.E.	1955 J. Chem. Soc. 1734.
1.31	Wright H.	1962 unpublished. Rhodes University.
1.32	Mathieson A., Robertson J.M. and Sinclair V.C.	1950 Acta. Cryst. 3 245.
1.33	Sharn C.	1961 J. Chem. Phys. 34 1.
1.34	Bree A. and Lyons L.E.	1956 J. Chem. Phys. 384.
1.35	Birks J.B. and Christophorou L.G.	1962 Nature 196 4849.
1.36	Lyons L.E.	1955 J. Chem. Phys. 23 220.
1.37	Chynoweth A.G.	1954 J. Chem. Phys. 2 6.
1.38	Alexander P.W., Lacey A.R., and Lyons L.E.	1961 J. Chem. Phys. 34 2200.
1.39	Shpak M.T. and Sheka E.F.	1960 Optics and Spectroscopy 8 1.

1.40	Bowen E.J., Mikiewicz E. and Smith F.W.	1949 Proc. Phys. Soc. A62 349.
1.41	Prikhot'ko A.F. and Fugol' I.	1958 Optics and Spectroscopy 4 335.
1.42	Prikhot'ko A.F. and Fugol' I.	1959 Optics and Spectroscopy 7 1.
2.1	Frey A.R.	1936 Phys. Rev. 49 305.
2.2	Hamilton T.D.S.	1961 Proc. Phys. Soc. 78 5 503.
2.3	Loeb L.B.	1939 Fundamental Processes of Electronic Discharges in Gases. Wiley and Sons.
2.4	Luhr O. and Bradbury N.E.	1931 Phys. Rev. 37 998
2.5	Craggs J.D. and Meek J.M.	1946 Proc. Roy. Soc. 1005 186.
2.6	Slack F.G.	1926 Phys. Rev. 28 1.
2.7	Rayleigh, Lord	1944 Proc. Roy. Soc. A 183 26.
2.8	Hamilton T.D.S.	1956 M.Sc. Thesis. Rhodes University
3.1	Sabine G.B.	1939 Phys. Rev. 55 1064.
3.2	Tanaka Y., Jursa A.S. and Le Blanc F.J.	1958 J. Opt. Soc. Am. 48 5.
3.3	Elmore W.C. and Sands M.	1949 Electronics. McGraw Hill.
3.4	East L.V. and Parker W.E.	1960 Rev. Sci. Inst. 31 11.
4.1	Packer D.M. and Lock C.	1951 J. Opt. Soc. Am. 41 10 699.
5.1	Engstrom R.W.	1947 J. Opt. Soc. Am. 37 6.
5.2	Platt	1954 M.Sc. Thesis. Rhodes University
5.3	Wiggins C.S. and Earley K.	1962 Rev. Sci. Inst. 33 10.

5.4	Bell D.A.	1960 Electrical Noise v. Nostrand Publishers.
5.5	de Jager G.	1958 Honours Project Rhodes University.
5.6	Birks J.B. and Little W.A.	1953 Proc. Phys. Soc. A 66 10.
5.7	Berton A.	1939 Comptes Rendus 208 1898.

TABLE 1 Principal Maxima in Absorption Spectrum of Anthracene.

3920	3700	3520	3330				: crystalline film	(1.)
3915	3700	3510	3340	3190			: vapour	(2.)
	3790	3570	3390	3160	2580	2200 1870	: in n-heptane	(3.)
	3760	3550	3390	3240			: in cyclo-hexane	(4.)
	3800	3590	3420	3260			: in toluene	(4.)

Wavelengths in Angstrom Units.

TABLE 2 Principal Maxima in Fluorescence Spectrum of Anthracene

4673	4425	4184	3984				: micro-crystals	(5.)
	4450	4200	3975				: in cyclo-hexane	(4.)
		4150			3600		: micro-crystals	(6.)
4707	4425	4176	4024	3802			: micro-crystals	(7.)

Wavelengths in Angstrom Units.

TABLE 3 Wavelengths in Angstrom Units.
Principal Minima in Excitation Spectrum of Anthracene.

3968	3745	3546	3367	3226			: 001 face	(5.)
					2220	1910 (1650 1510)	: 001 face fine structure	(8.)

Principal Maxima in Excitation Spectrum of Anthracene.

3120	3075	3005	2950	2860	2810	2760	2710	2470	: 001 face	(8.)

TABLE 4 Principal Maxima in Reflection Spectrum of Anthracene.

3920	3700			2700	2600	2500	2240	: 001 crystal face (9.)
	3750	3535	3375	2830				: powder (10.)

Wavelengths in Angstrom Units.

1. Kortum & Finckh (1.22)
2. Seshan (1.23)
3. Klevens & Platt (1.24)
4. de Jager (5.5)
5. Wright G.T. (1.10)
6. Birks & Little (5.6)
7. Birks & Wright (1.2)
8. Driver (1.17)
9. Wright H. (1.31)
10. Berton (5.7)

TABLE 5 Recombination Coefficients (2.4)

Gas	Coeff. 'a' x 10^{-6}
Oxygen	1.32
Nitrogen	1.06
Argon	1.06
Hydrogen	0.28
Air	1.23

TABLE 6 Optical Dimensions of Spectrograph.

Distance of entrance slit from mirror = 40 cms.
Distance of exit slit from mirror = 80 cms.
Radius of Curvature of Mirror = 56 cms.

Wavelength A.U.	3000	2500	2000	1500	1400
Dispersion mm./A.U. x 10^{-3}	2.8	5.2	11.5	40	67
Reciprocal Dispersion	360	190	87	25	15
Wavelength Range A.U. (Slit width = 0.1 cm.)	36	19	8.7	2.5	1.5

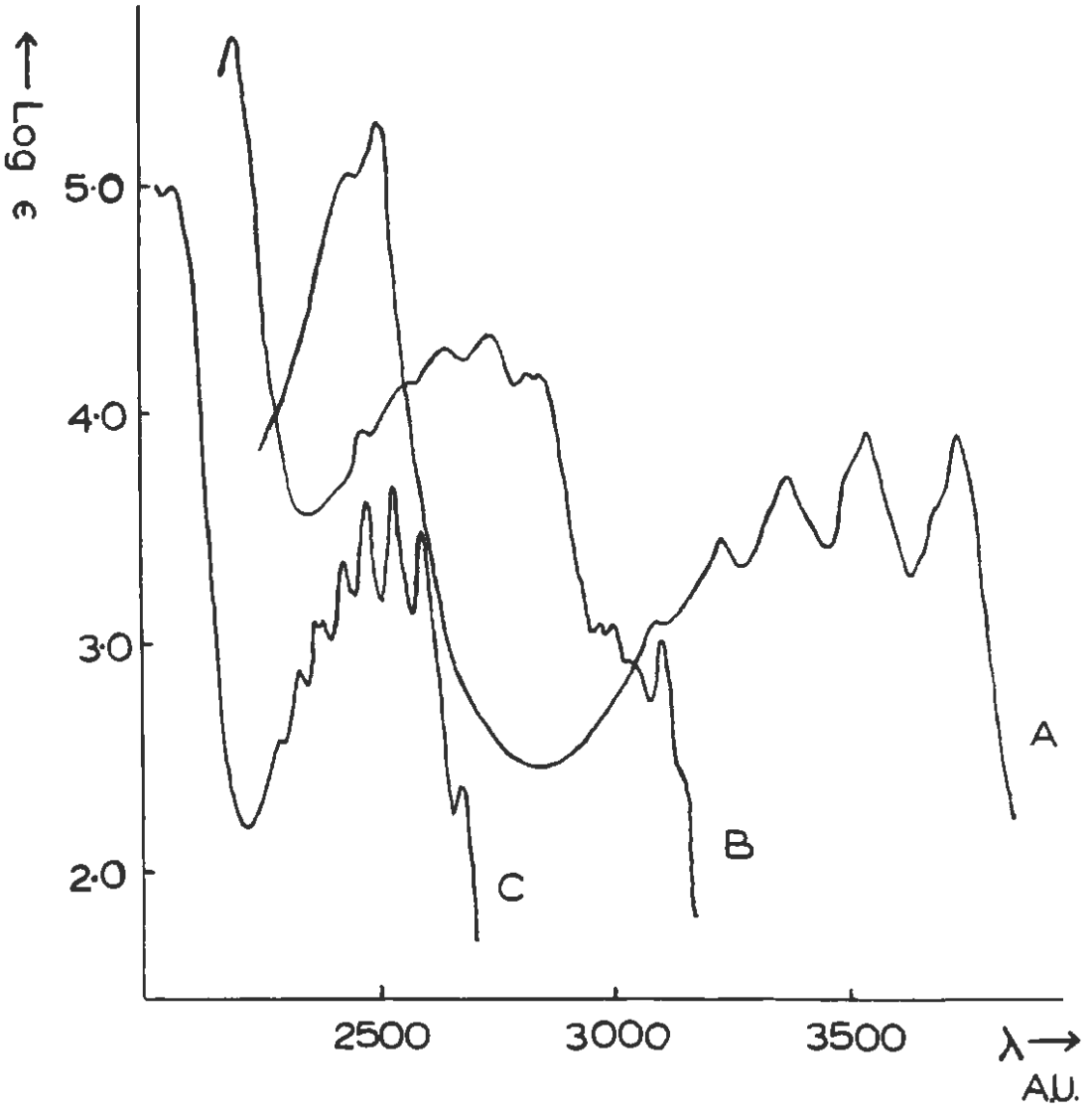

FIGURE 1. Absorption Spectra (1·25)

A. Anthracene
B. Naphthalene
C. Benzene

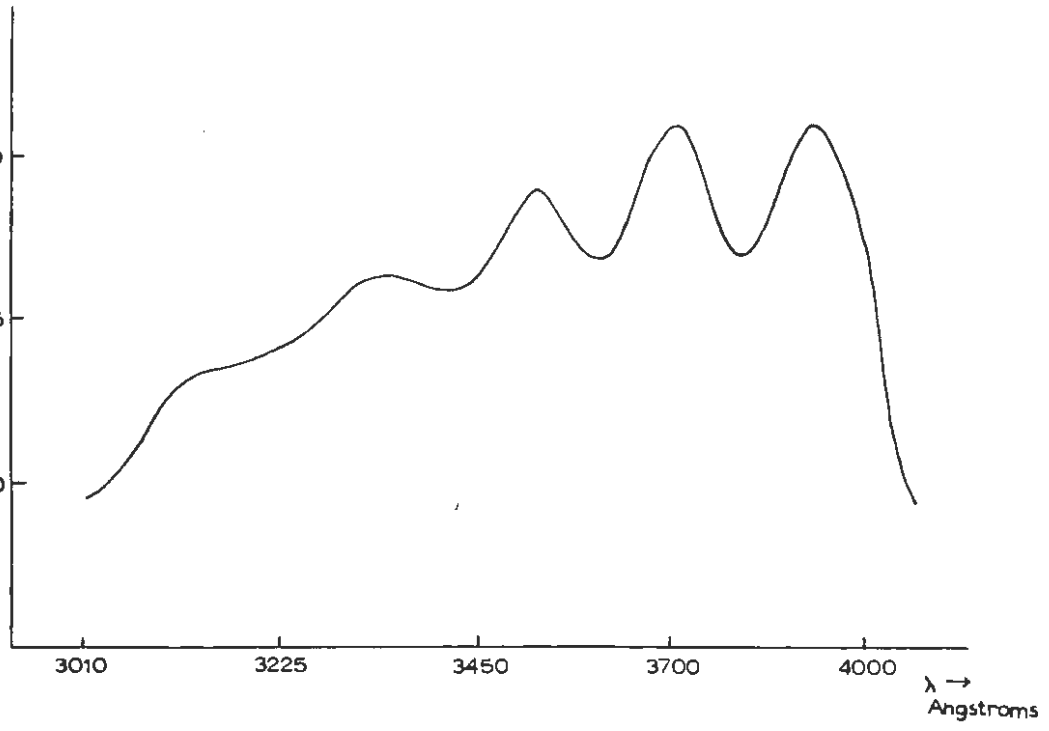

FIGURE 2. Absorption Spectrum of Anthracene (1.22)

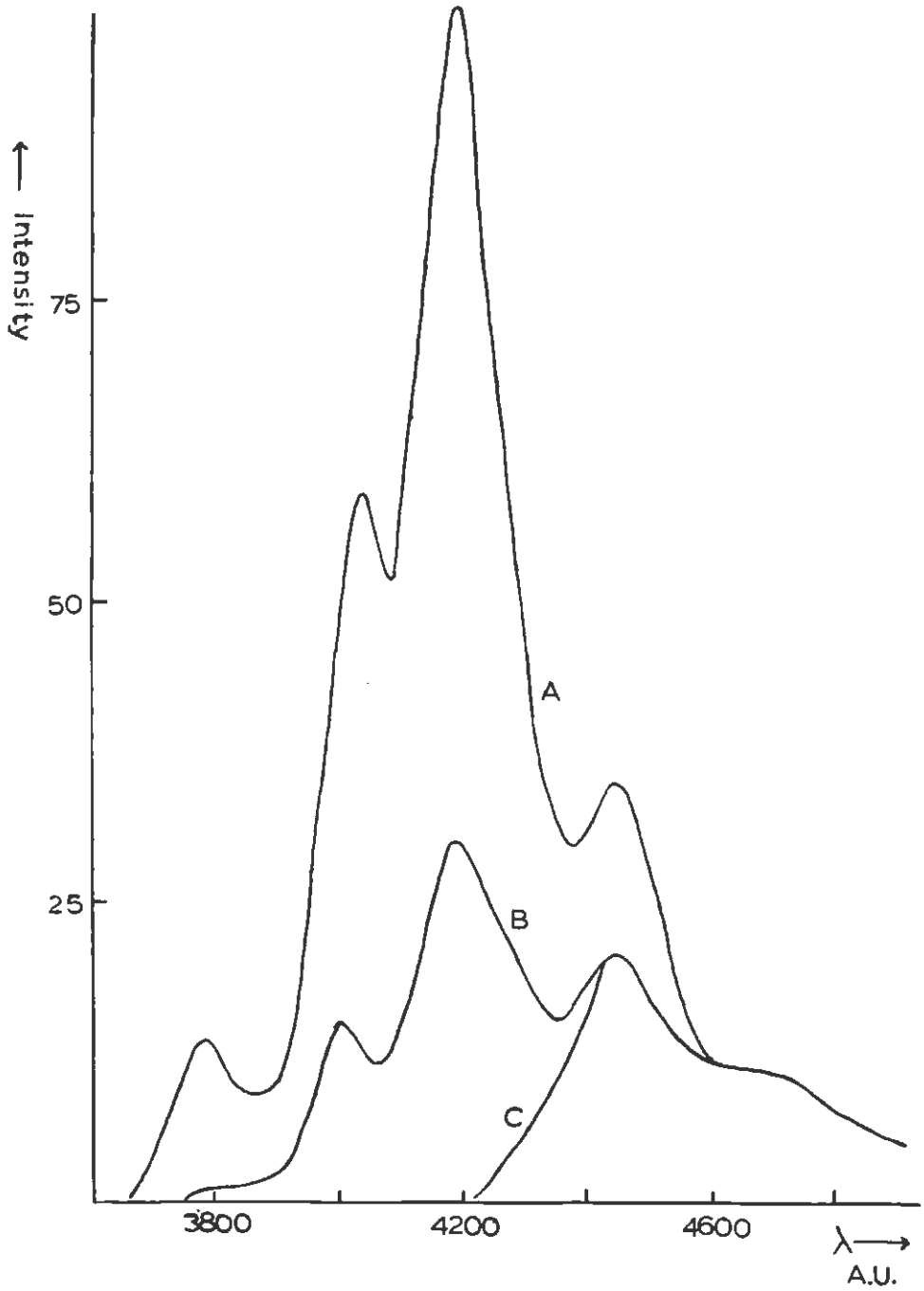

FIGURE 3. Fluorescence of Anthracene (1·26)

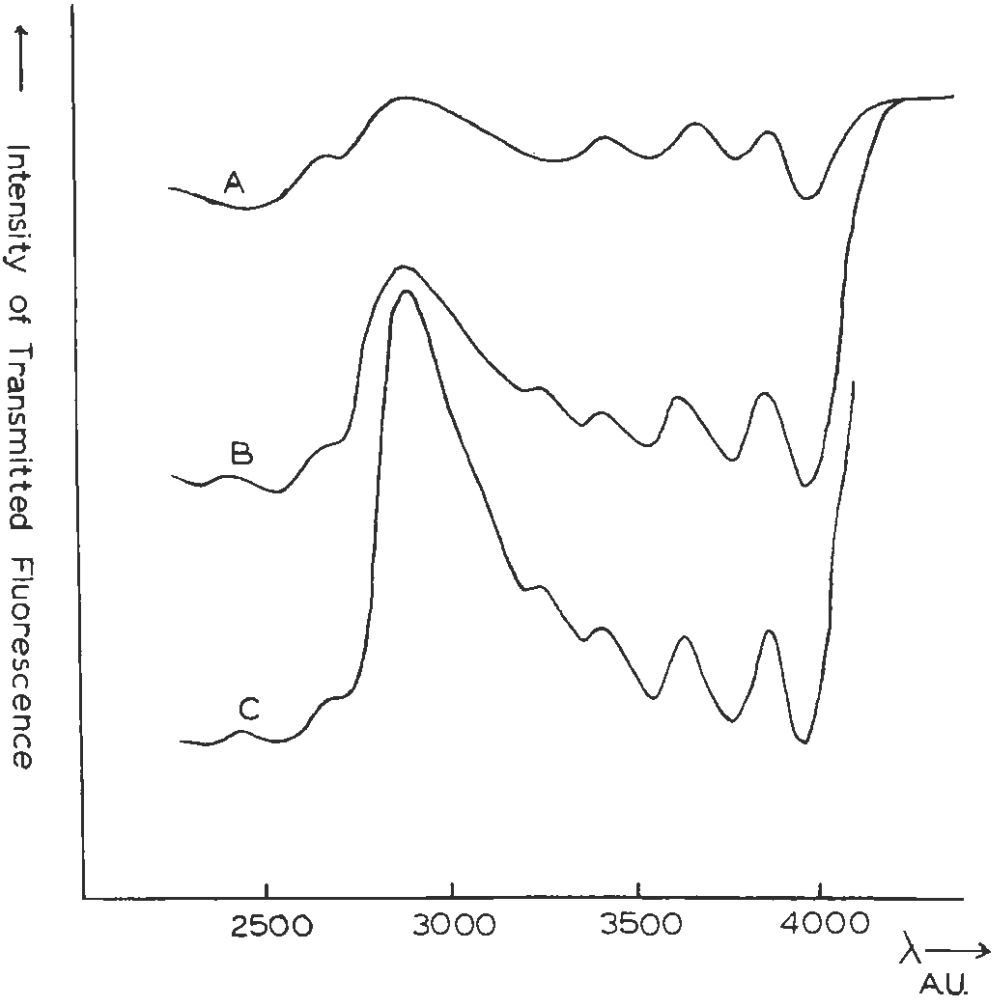

FIGURE 4. Excitation Spectra of Anthracene (1·16)

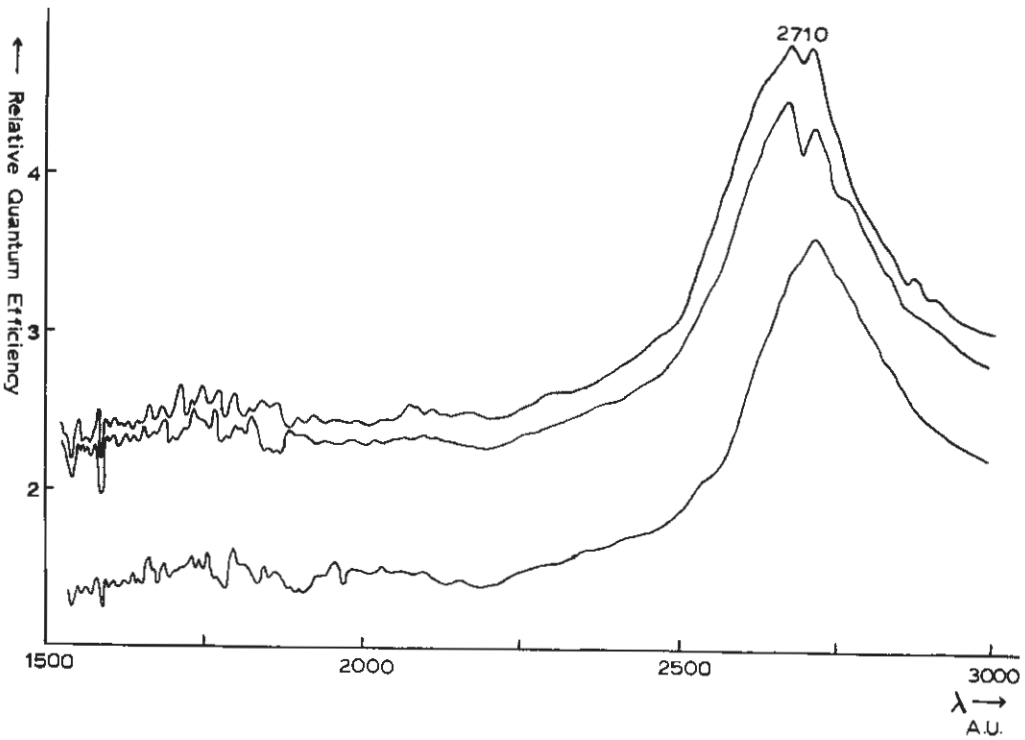

FIGURE 5. Excitation Spectrum of Anthracene (1·17)

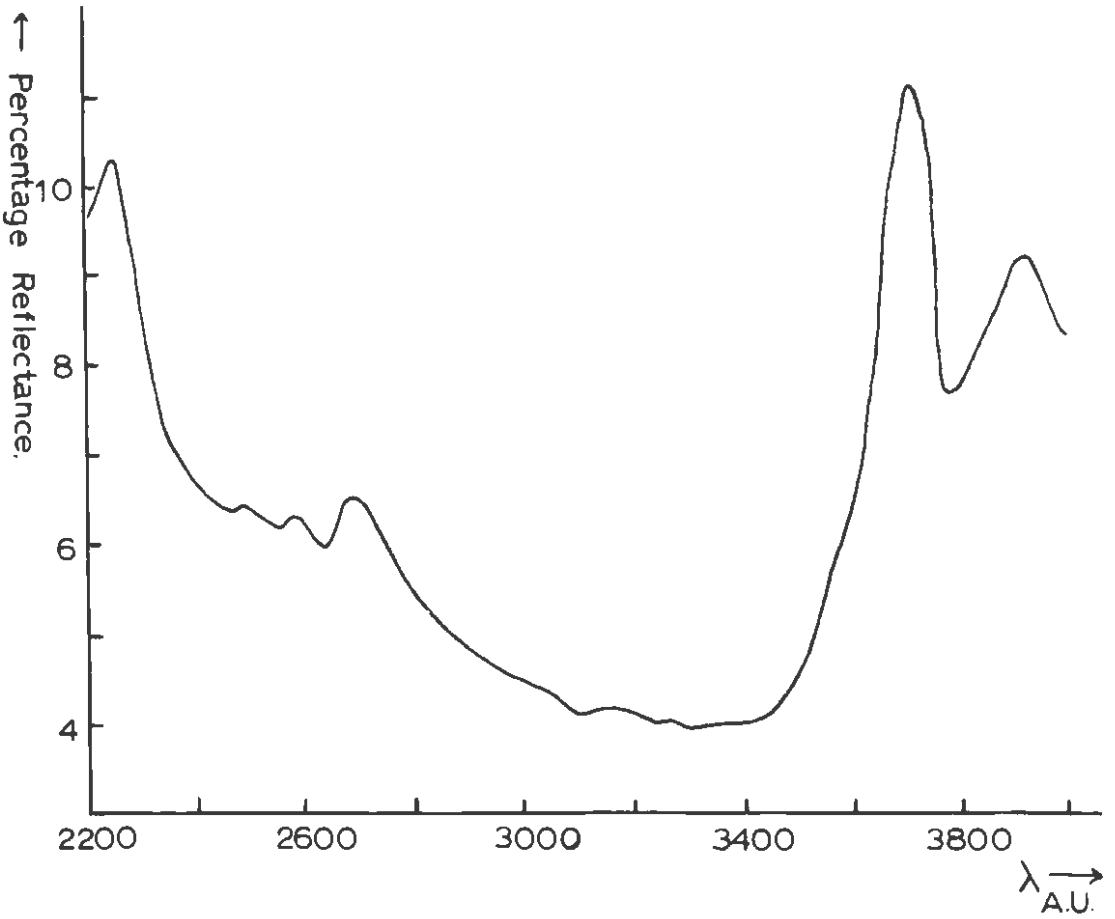

FIGURE 6. Reflection Spectrum of Anthracene (1·31)

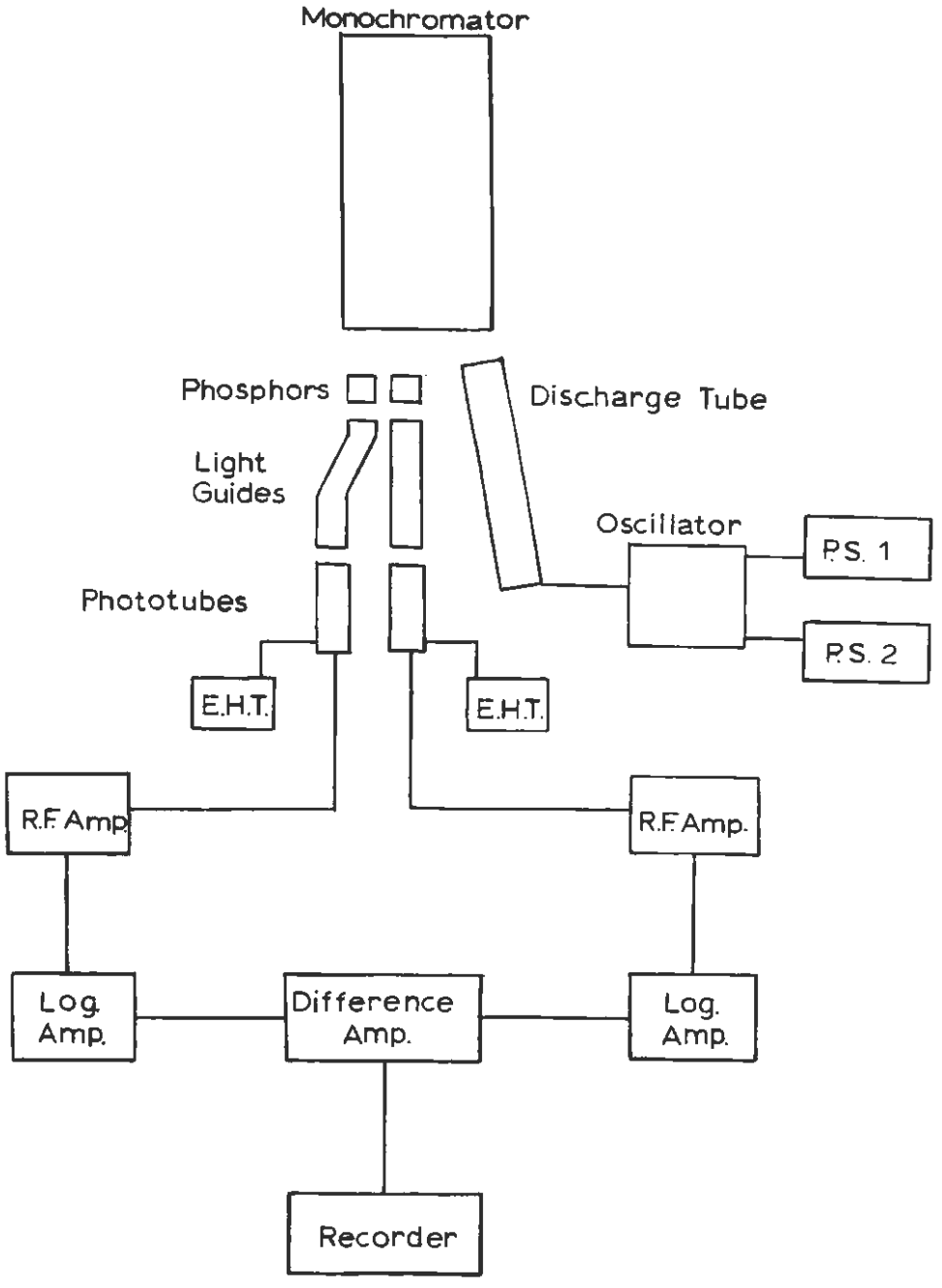

FIGURE 7. Block Diagram of Apparatus

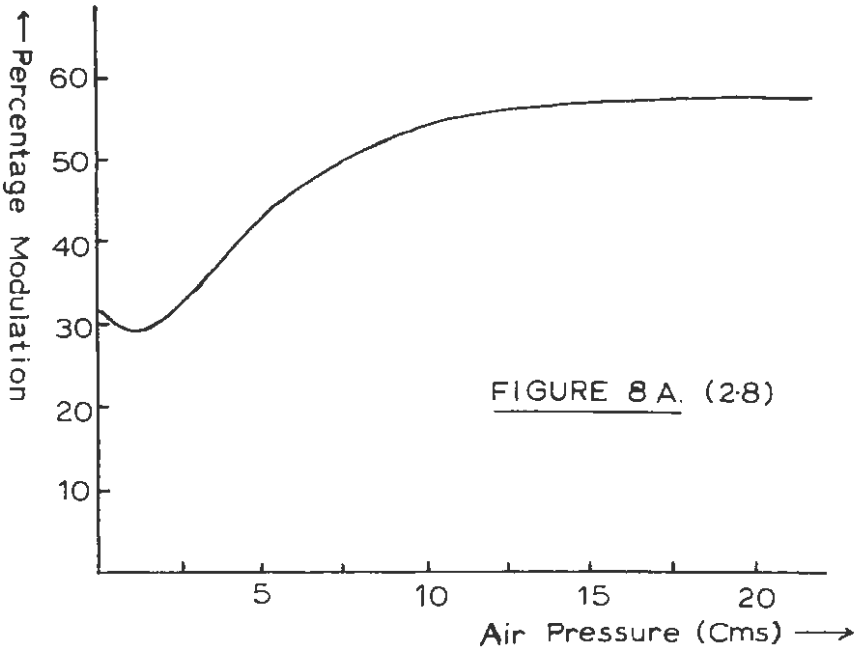

FIGURE 8 A. (2·8)

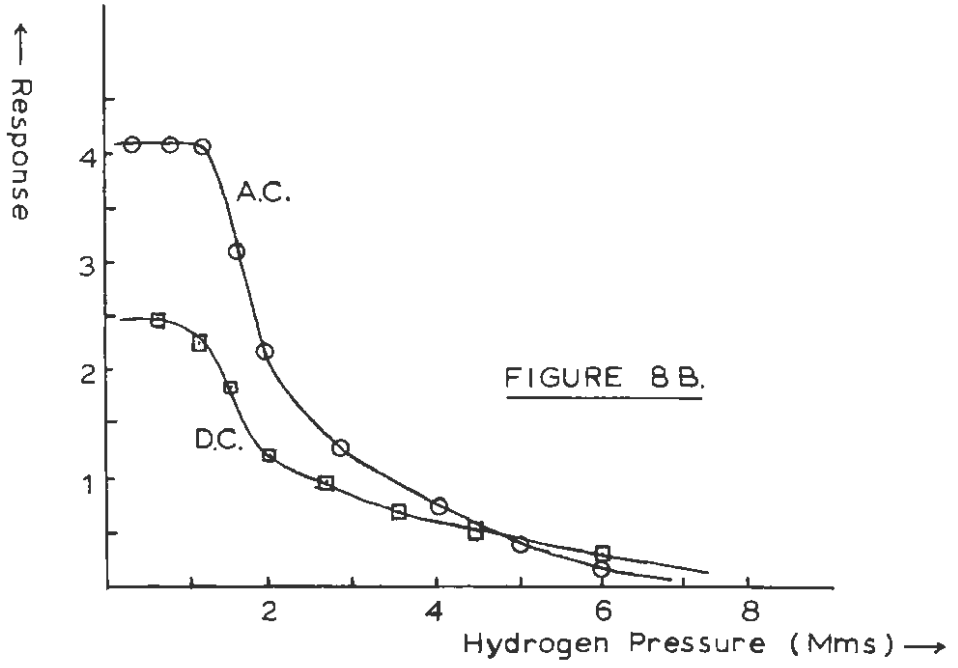

FIGURE 8 B.

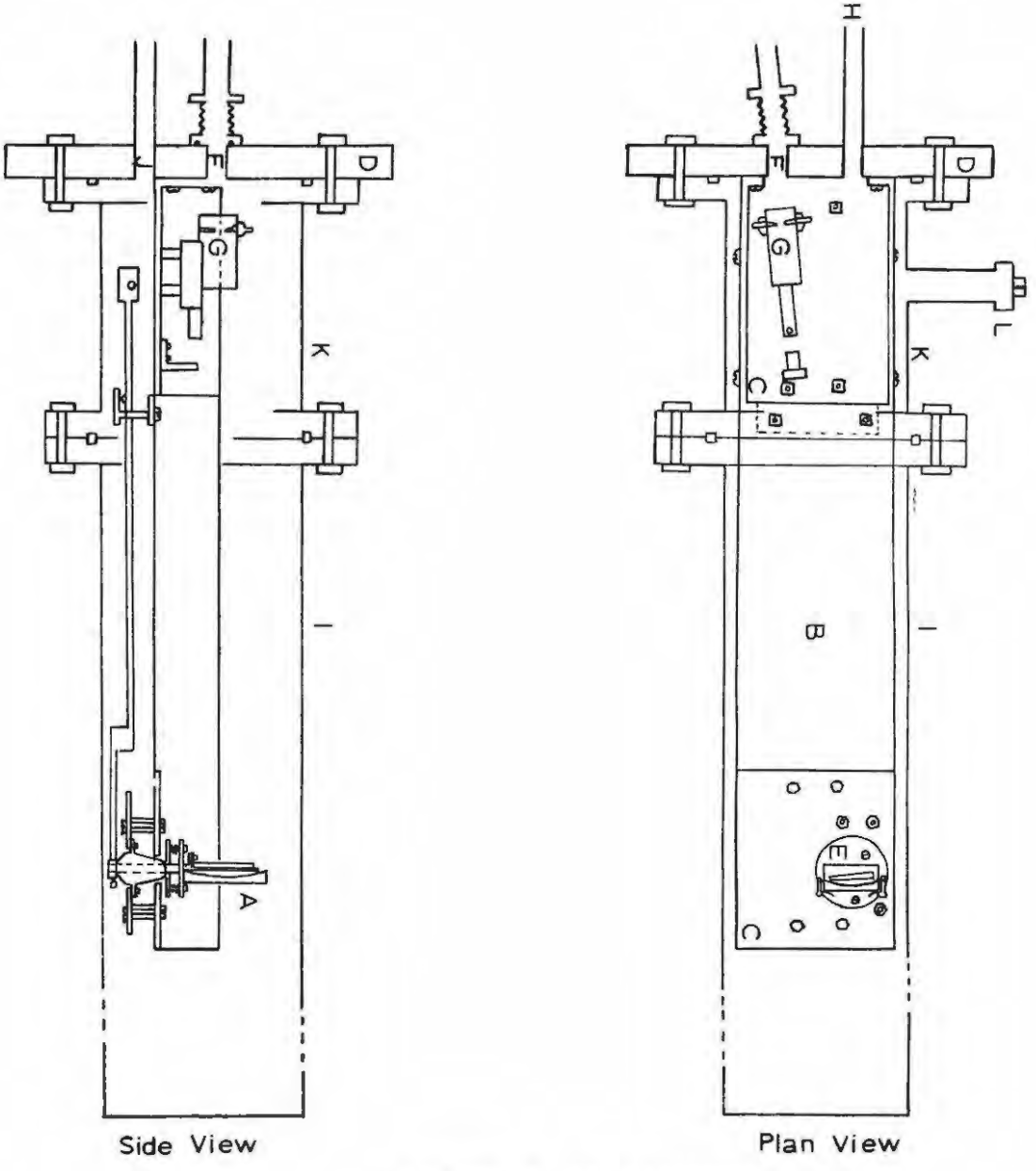

FIGURE 9. The Monochromator

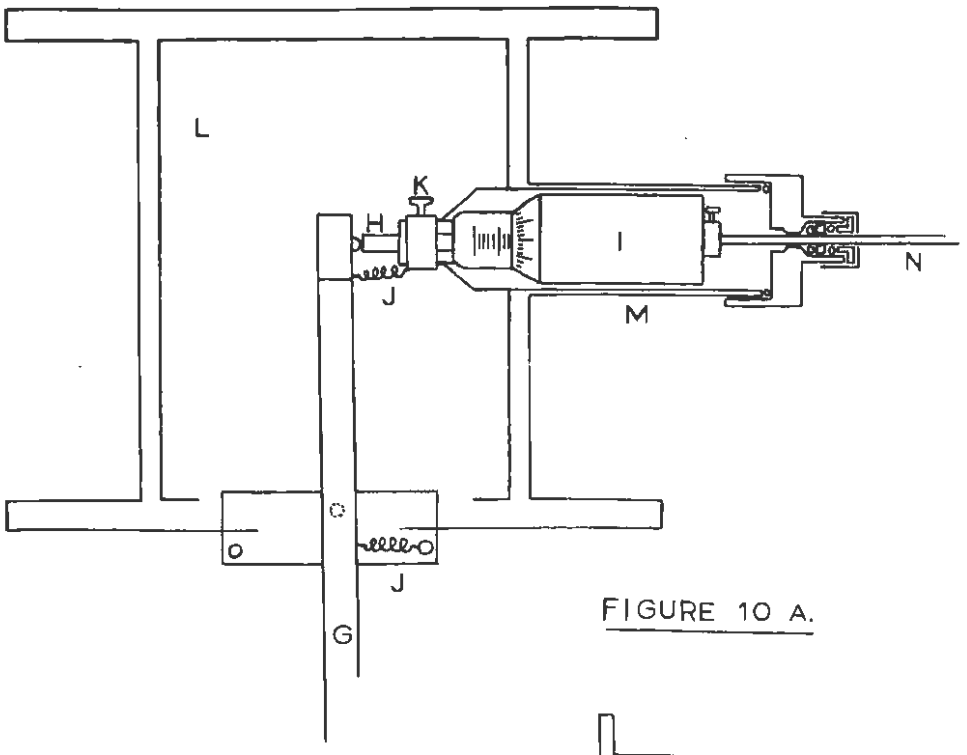

FIGURE 10 A.

FIGURE 10 B.

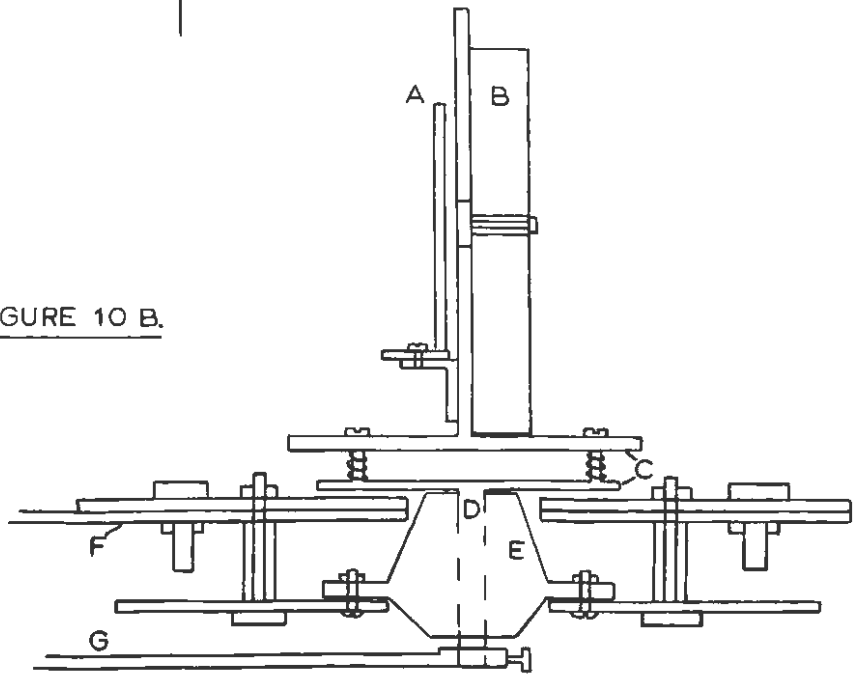

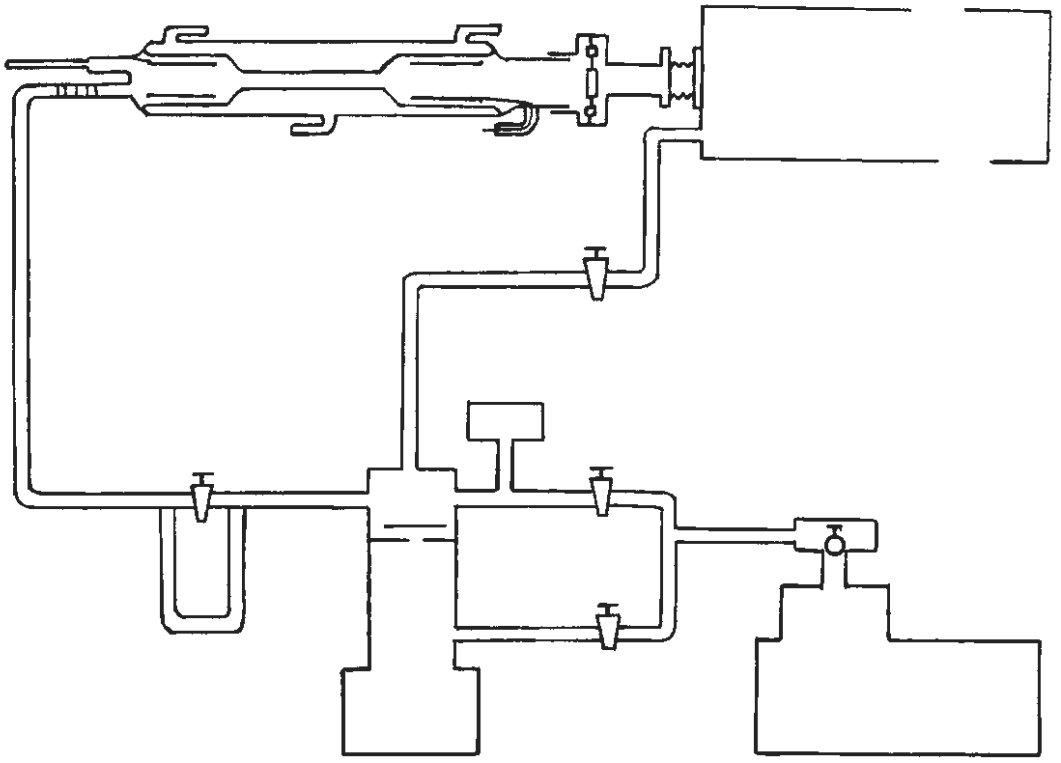

FIGURE 11. The Vacuum System

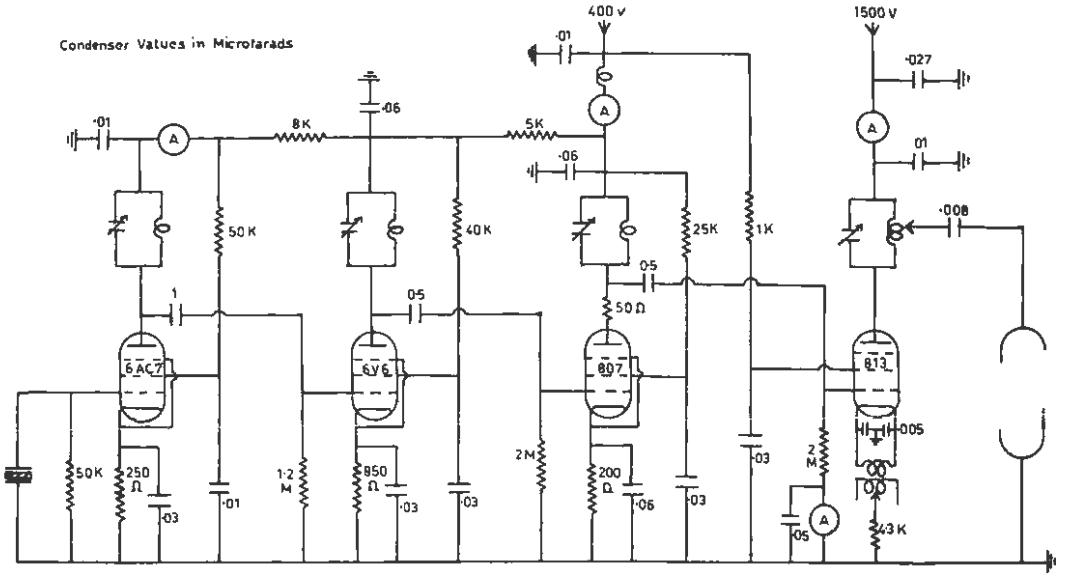

FIGURE 12 Power Oscillator

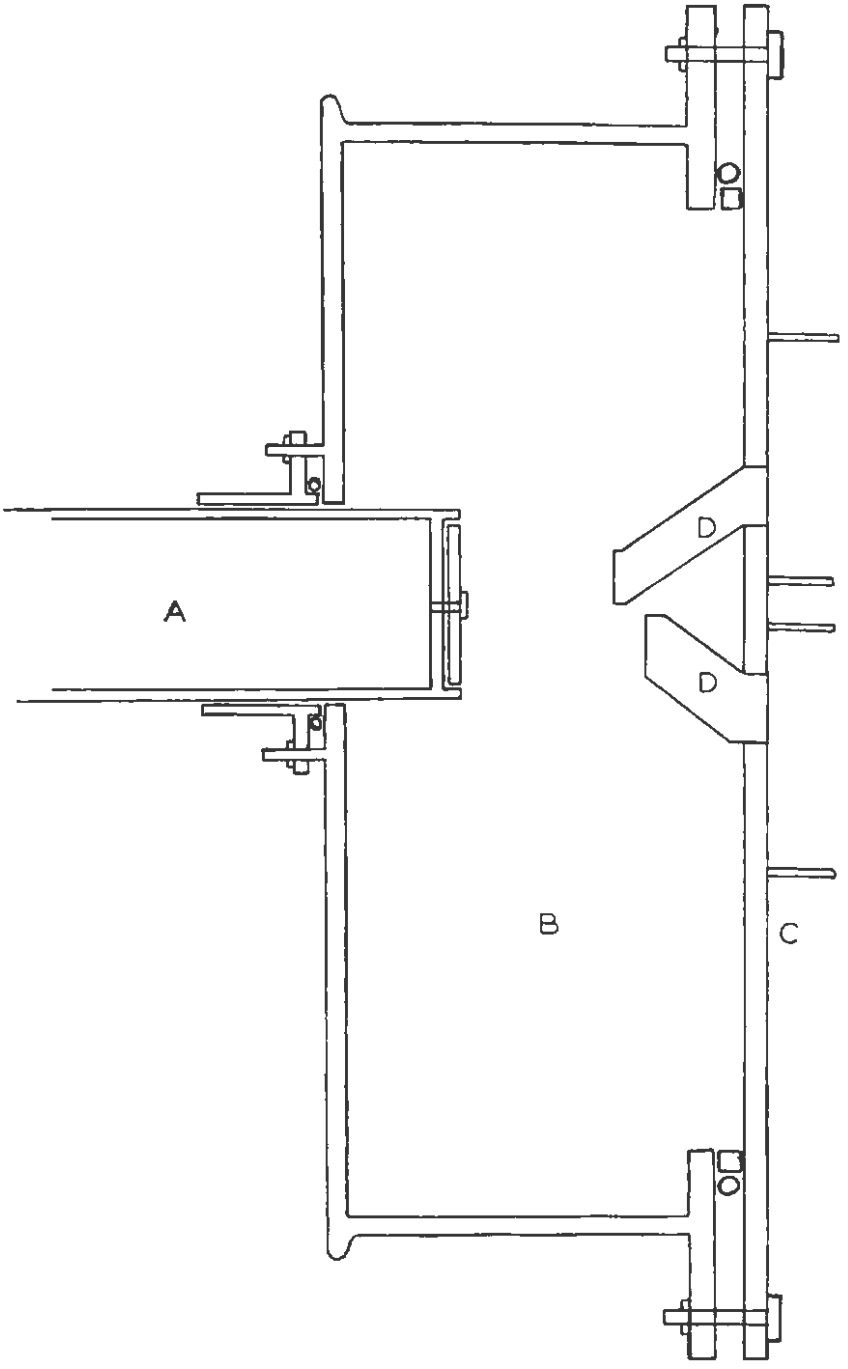

FIGURE 13. The Sample Chamber

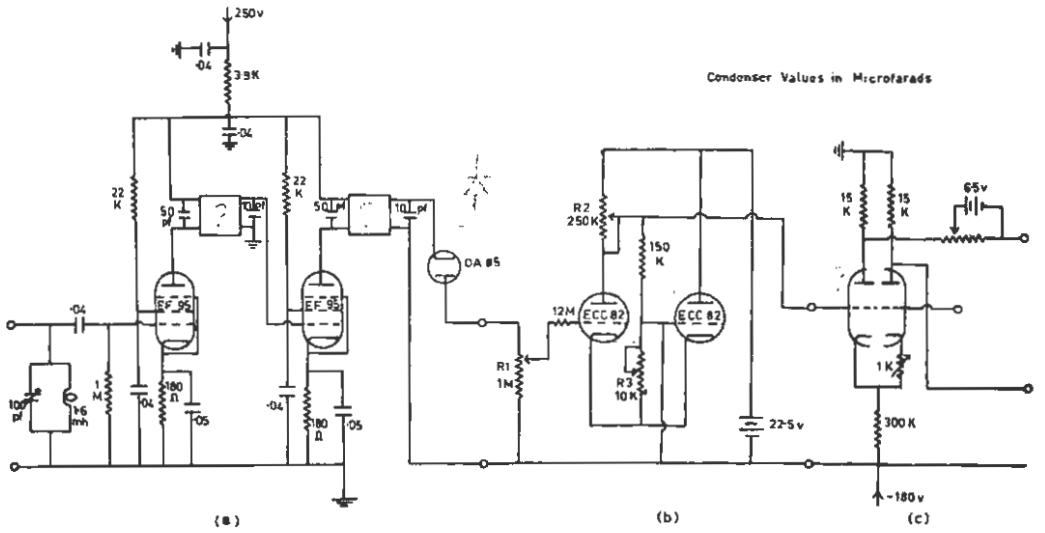
250v
·04
39K
·04
22 K
50 µµF
22 K
50 µµF
10 µµF
DA 85
EF 95
EF 95
·04
180 Ω
·05
·04
180 Ω
·05
1 M
·02
R1 1M
12M
ECC 82
ECC 82
R2 250K
150 K
R3 10K
22·5v
15 K
15 K
65v
1 K
300 K
-180v
Condenser Values in Microfarads
(a)
(b)
(c)

FIGURE 14

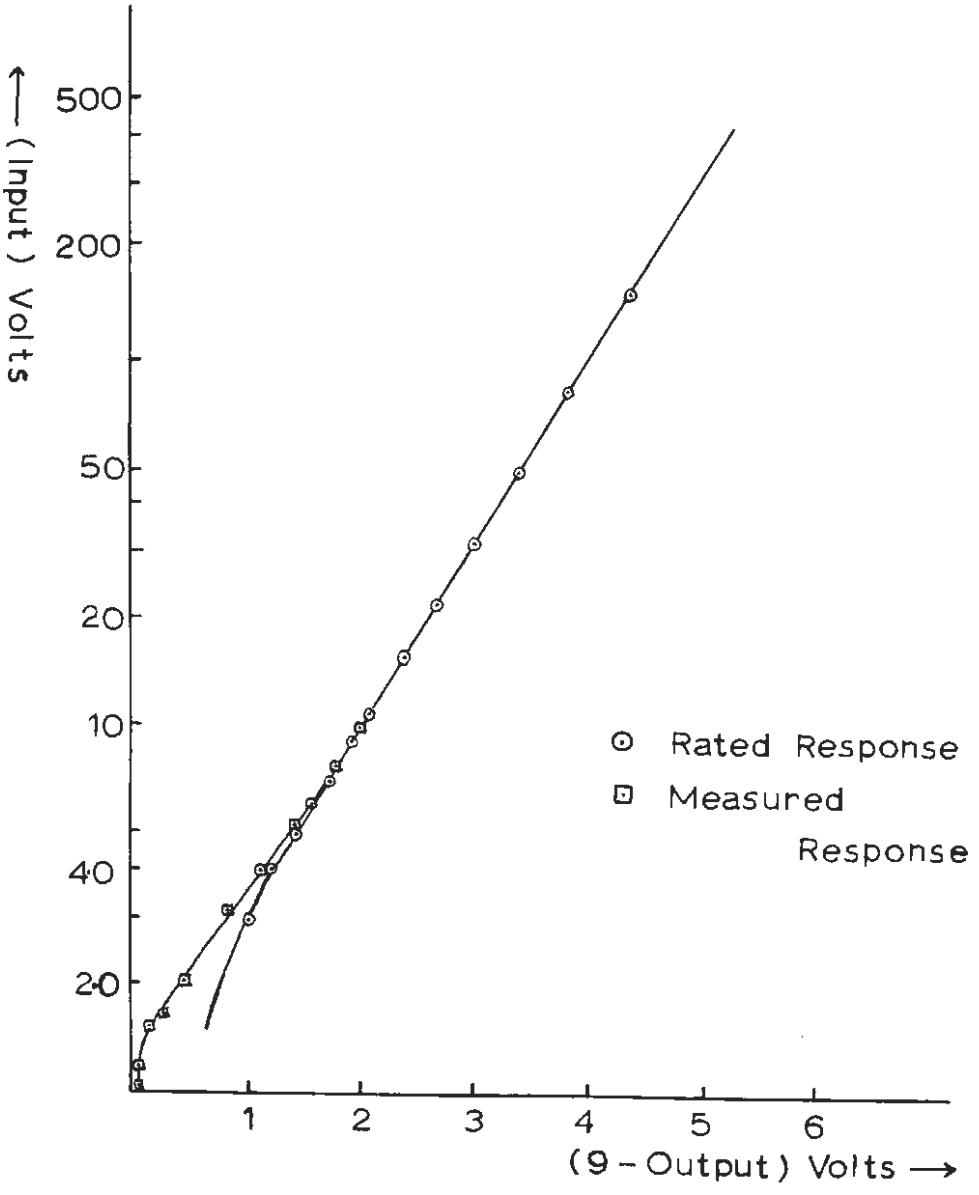

FIGURE 15. Log Amplifier Characteristics

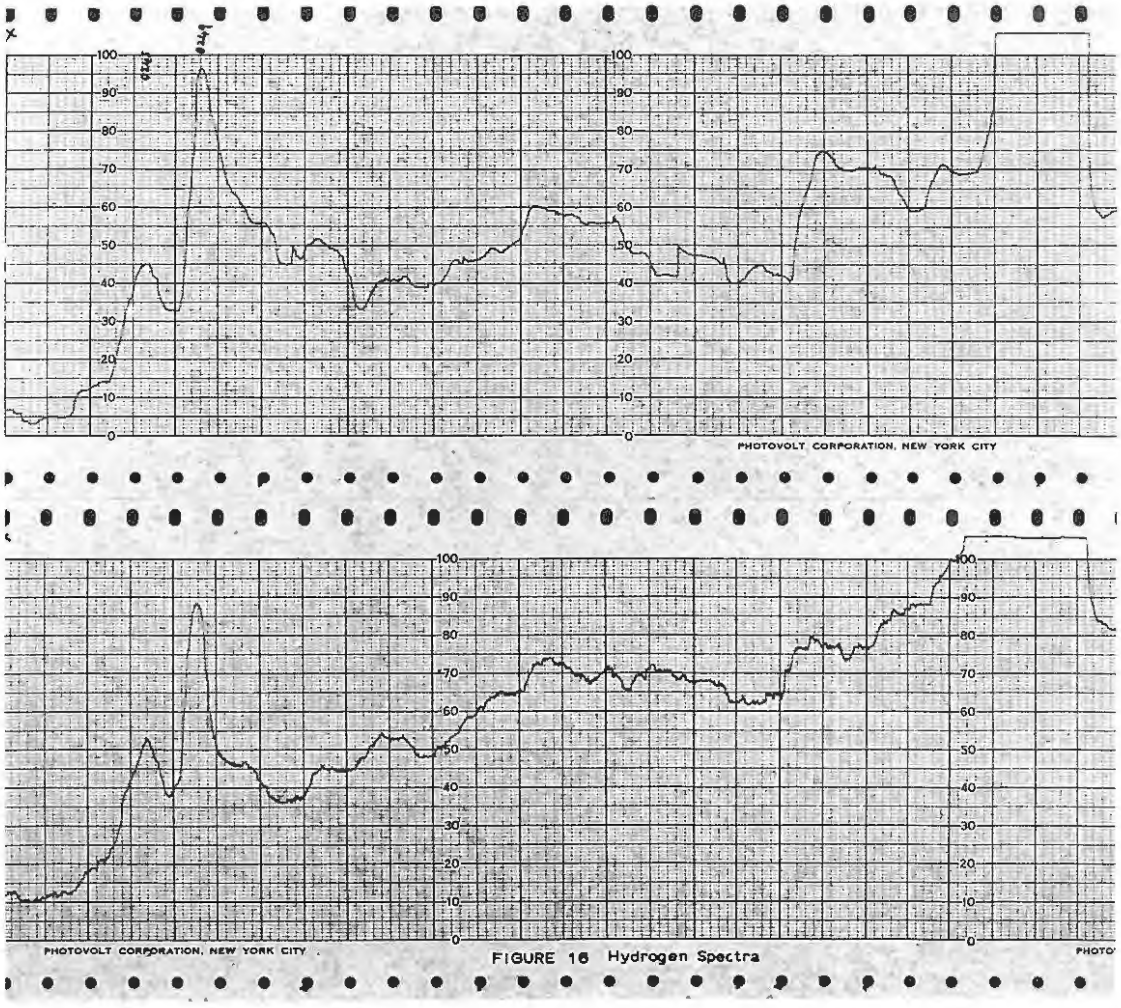

FIGURE 16 Hydrogen Spectra

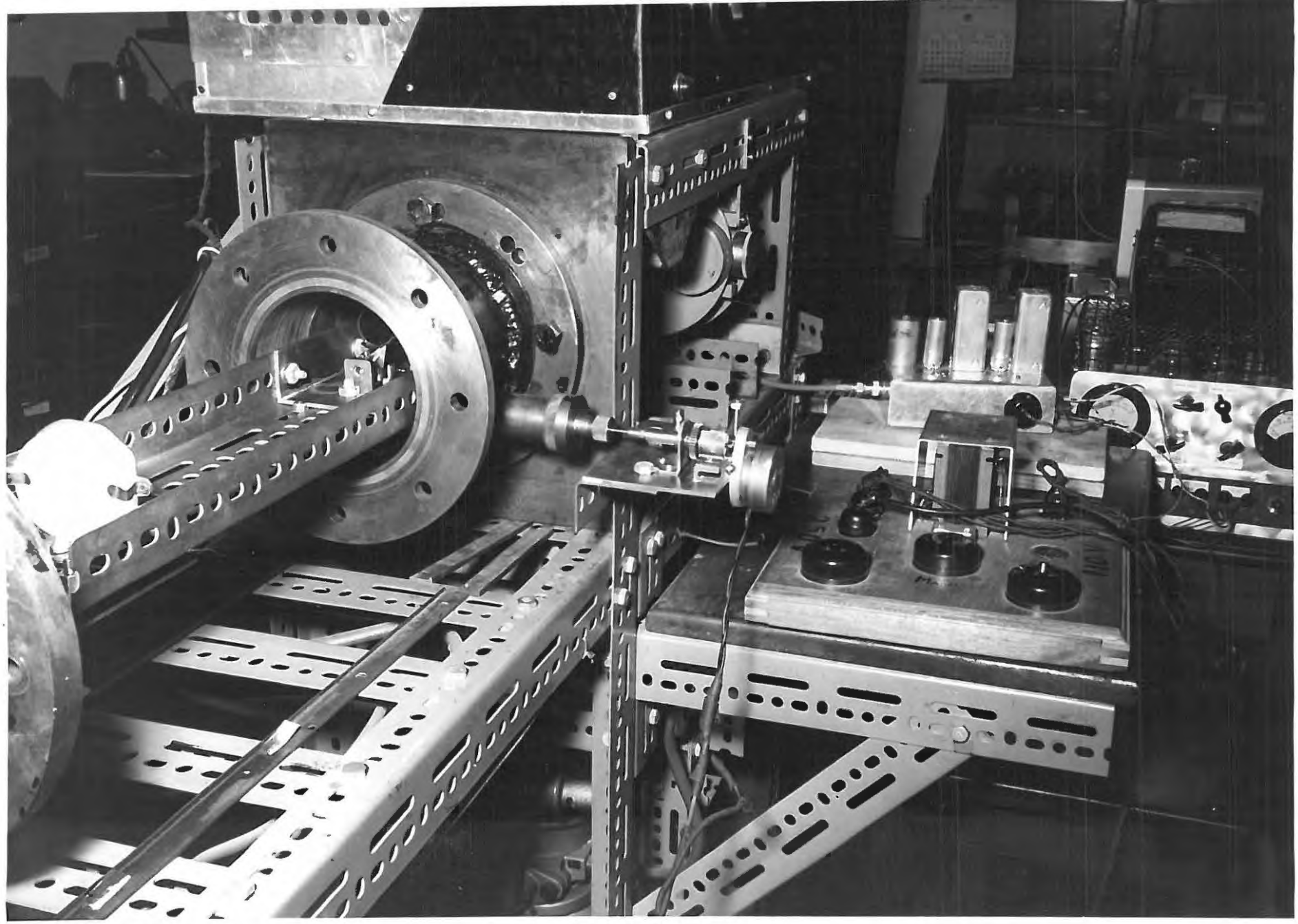

PLATE 1

PLATE 2